

For each 40-day period between successive moves of observers, the number,  $N$ , of observations showing cloudiness not greater than 2 (or not greater than 4) was found for each observing station. Next, an arithmetical mean  $\bar{N}$  of values  $N$  for particular stations was computed for each 40-day period. Indices  $k = 100 \bar{N}/\bar{N}$ , expressing the number of observations at the time of which there was a degree of cloudiness not greater than 2 (not greater than 4, respectively) at a given station in relation to the average number of such observations made at all stations in a given 40-day period, were found.

In compiling the results of cloudiness observations, the systematic differences between observers are clearly noticed. Two observers always remained at each station. Accordingly, the values of systematic deviations from the mean could be computed only for pairs of observers. A weighted mean value of  $k$  was computed for every pair of observers without regard to the stations at which the particular pair was at a given time. The quantities  $\bar{N}$  for respective periods were taken as weights. The weighted mean value thus obtained is:

$$\bar{k} = 100 \frac{\sum_{i=1}^n N_i}{\sum_{i=1}^n \bar{N}_i}, \quad (1)$$

where  $n$  is the number of all 40-day periods (in this case  $n=17$ ).

In order to eliminate the systematic differences between observers, all values  $N$  were divided by values  $\bar{k}$  relating to particular pairs of observers. From the values  $N' = N/\bar{k}$  obtained in this way for respective posts in a given 40-day period, weighted mean values  $\bar{N}'$  were formed and the indices  $k' = 100 \bar{N}'/\bar{N}'$  were computed. The weighted mean  $\bar{k}'$  of values  $k'$  for a given station, where the values  $\bar{N}'$  were taken as weights, can be found from the formula

$$\bar{k}' = 100 \frac{\sum_{j=1}^n N'_j}{\sum_{j=1}^n \bar{N}'}. \quad (2)$$

The values  $\bar{k}'$ , obtained in this way, can be treated as indices of the number of clear nights at particular stations free from systematic differences between observers. These are given in Table 2.

The indices of individual observations of cloudiness not greater than 2, are given in column 2 of Table 2, while those of cloudiness not greater than 4 in column 3. Similar indices for cases where both observations carried out on the same night showed cloudiness not greater than 2, or not greater than 4, are given in column 4, or in column 5, respectively. The bottom line of Table 2 gives the percentage frequency of the observations during which a given degree of cloudiness was noted as an average for all stations.

Each observation of cloudiness was complemented by a check as to the visibility of the Pole Star. The indices for these sightings are given in column 8 of Table 2.

The estimate of cloudiness was influenced by the degree to which the horizon was obscured at a given station. The percentage of the celestial sphere covered by trees, hills, etc., up to  $15^{\circ}$  over the horizon, is approximately 10 per cent in Mała Wieś, Reducin and Wola Rafałowska, whereas it is 45 per cent in Ostrowik. In order to eliminate this effect, apart from conventional observations of cloudiness after October 1954 only the cloudiness of the part of the celestial sphere more than  $15^{\circ}$  above the horizon was estimated. The indices obtained from these observations are given in column 6 of Table 2 where no cloud was present during both observations on a given night and in column 7 for cloudiness not greater than 2.

Table 2.  
Number of clear nights (indices).

	Individual ob-servation of the whole sky	Both observations of the whole sky on one night	Both observations of the sky above $h = 15^{\circ}$ on one night	Pole star visible
Mała Wieś	$C \leq 2$ $C \leq 4$	$C \leq 2$ $C \leq 4$	$C = 0$ $C \leq 2$	
Ostrowik	$102 \pm 2$ $97 \pm 2$	$101 \pm 9$ $91 \pm 6$	$102 \pm 9$ $99 \pm 7$	$97 \pm 3$
Reducin	110 2 105 3	106 8 103 4	92 7 98 3	103 3
Wola Rafałowska	91 3 99 2	93 7 95 4	90 8 97 4	101 2
Percentage frequency	101 3 100 2	103 5 103 4	114 6 106 4	101 2
	21	30	15	37
	22		9	
			14	

The results given in Table 2 show that there are no significant differences in cloudiness between the observing sites.

### Wind

Wind velocity was measured twice during the night, at the same time as the cloudiness observations, using Robinson anemometers placed at a height of 2.5 meters above ground level. The results are presented in Table 3, showing the percentage frequencies of observations giving different wind velocities.

Table 3.  
Wind velocity (percentage frequency).

	$\bar{v}$ (m/sec.)	$v \leq 0.3$	$0.3 \text{ to } 1.0$	$1.0 \text{ to } 2.0$	$v > 2.0$
Mała Wieś	1.35	24	24	24	28
Ostrowik	1.41	21	24	28	28
Reducin	1.83	15	20	29	36
Wola Rafałowska	1.51	27	18	25	31

Wind velocity depends to a very large extent on the season. A test of the hypothesis that the mean wind velocity is the same at all sites, therefore proved positive. The hypothesis that there is no difference between the sites in mean values of wind velocity after eliminating the systematic seasonal deviations was therefore also tested. For this purpose, mean values  $v$ , of wind velocity for respective 40-day periods were computed and the mean value,  $\bar{v}$ , for the whole two years of observations; the data from all observing stations were treated as a whole. The difference,  $\bar{v} - v$ , between these values was regarded as a seasonal correction which had to be added to the mean values of wind velocity for particular observing stations in a given 40-day period.

The result of testing our hypothesis by methods of analysis of variance gave grounds for rejection of this hypothesis, namely the value of Fisher's  $Z$  parameter\*) computed from the observational data corrected in the way mentioned above, is 0.65, whereas the value of the  $Z$  parameter for the corresponding number of degrees of freedom of the level 0.05 is 0.51.

This means that there are significant differences in wind velocity between the observing sites: the smallest mean wind velocity being in Mała Wieś and the highest in Reducin.

### Humidity and temperature

Air temperature and humidity were measured twice during the evening, at the same time as the observations of cloudiness. Humidity was measured with an Assman-type psychrometer. There was found to be no difference in humidity and temperature between the different observing sites. Thus, for instance, the mean percentage humidity was  $86 \pm 2$  in Mała Wieś,  $87 \pm 2$  in Ostrowik,  $85 \pm 1$  in Reducin, and  $87 \pm 1$  in Wola Rafałowska — whereas the percentages of observations showing humidity greater than 88 per cent, were  $49 \pm 8$  in Mała Wieś,  $55 \pm 8$  in Ostrowik,  $46 \pm 5$  in Reducin, and  $50 \pm 4$  in Wola Rafałowska.

### Glare

The brightness of the glare visible over the horizon was estimated on a 3-degree scale on each moonless night at 9 p. m. and at midnight, local time (in summer at midnight only). Table 4 gives the percentage frequency of observations showing bright, weak or no glare. Only the estimates made at a cloudiness of less than 2 were taken into account; the total number of such estimates is denoted by  $n$ .

The reason for the appearance of glare is the proximity of an observing station to a town or to an industrial plant. Thus, the majority of the brightest glare observed from Ostrowik appeared over

---

\*) See e. g. Fisher, R. A. *Statistical Methods for Research Workers*, Edinburgh-London, 1941.

Table 4.  
Glare (percentage frequency).

	bright	weak	nil
Mała Wieś (n = 142)	9	15	76
Ostrowik (n = 123)	13	33	54
Reducin (n = 177)	6	21	73
Wola Rafałowska (n = 202)	31	20	49

Warsaw, and from Wola Rafałowska over the nearby town of Mrozy. Owing to its location the greatest amount of bright glare was observed from Wola Rafałowska, the smallest from Reducin.

#### Quality of star images

On every clear night with cloudiness of not more than 5, the image quality of ten stars visible at various heights over the horizon was observed. Refracting telescopes 90 millimeters in diameter with a magnifying power of about 250x were used. The same stars were observed from all stations on a given night. The quality of the stellar diffraction images was estimated according to Pickering's scale\*).

Atmospheric turbulence, defined by Danjon and Couder\*\*) as the maximum angular deviation of a stellar light-ray from an average direction was deduced from each estimate of image quality. The scale according to which turbulence was deduced from the estimates, had been chosen in such a way that the ratio of turbulence to air mass was independent of the zenith distance. The scale of turbulence was made to agree with the values given by Danjon and Couder\*\*), e. g., the estimate 9a was assumed to correspond to turbulence 0''.37, the estimate 7a to 0''.77, the estimate 4 to 1''.46.

The values of turbulence obtained from the observations were reduced to the zenith by dividing them by the corresponding values of air mass. The air masses expressed in terms of the air mass at the zenith were taken from Bemporad's tables\*\*\*).

The altitude of the stars over the horizon was computed, taking into account the time of observation. For checking purposes the altitudes were, moreover, measured during the observations, with the use of a simple protractor.

The following equation was used in order to eliminate the systematic differences between the telescopes:

\* ) Pickering, E. C., *Harv. Ann.*, Vol. 61; see also: Mergenthaler, J., *A. A.* c 3, 1, 1936.

\*\*) Danjon, A., Couder, A., *Lunettes et telescopes*, 1935; ch. V.

\*\*\*) Bemporad, A., *Mitt. Heidelberg*, H. 4; 1904.

$$\Delta_k = \left[ \frac{1}{n^2} \sum_{i=1}^p \sum_{s=1}^l \alpha_{ik} \alpha_{is} \Delta_s \right] - \frac{1}{n} \sum_{i=1}^p \left( \bar{T}_i^* - T_{ik}^* \right). \quad (3)$$

Here  $\Delta_k$  is the correction to be subtracted from the values of the logarithms of turbulence obtained directly from the observations with a  $k$ -th telescope,  $n$  is the number of 40-day periods (in this case  $n=17$ ),  $p$  is the number of stations (in this case  $p=4$ ).  $l$  is the number of telescopes (in this case  $l=5$ ),  $\alpha_{ik}$  indicates how many times the  $k$ -th telescope was kept at the  $i$ -th station.  $\bar{T}_i^*$  is the mean logarithm of the observed turbulence at the zenith (without correction for the systematic error of the telescope (for the  $i$ -th 40-day period for all the stations.  $T_{ik}^*$  is the mean logarithm of the atmospheric turbulence at the zenith (without correction for the systematic error of the telescope) for the  $i$ -th 40-day period at the station, where the  $k$ -th telescope was in use.

We dealt with the logarithm of turbulence and not with turbulence itself because the error in determining atmospheric turbulence is in the first approximation proportional to the turbulence itself. The correction  $\Delta_s$  was computed from formula (3) by the method of successive approximations; in the first approximation, the term in the square bracket was taken as equal to zero. The corrections for systematic differences between the observers were similarly found.

The relative mean error of determination of the atmospheric turbulence at the zenith on the basis of estimations of the quality of the images of the ten stars is about 10 per cent. On the whole, about 5,000 estimates were made.

Mean logarithms of atmospheric turbulence at the zenith for the whole period of observation were used to find the mean values of the turbulence at the zenith given in Table 5:

Table 5.

## Turbulence at the zenith

Mała Wieś	$t_0 = 0''327 \pm 0''009$
Ostrowik	$0''338 \pm 0''008$
Reducin	$0''349 \pm 0''007$
Wola Rafałowska	$0''319 \pm 0''007$

Hence it can be seen that the quality of the star images at Wola Rafałowska and Mała Wieś was superior to that at the remaining stations. The differences between turbulence at the different stations were plainer still, when we compare the histograms of the distribution of atmospheric turbulence at the zenith for the particular sites (see Fig. 1).

It can be seen from these histograms that, for instance, at Wola Rafałowska on the average the atmospheric turbulence on every fourth clear night at the zenith did not exceed  $0''25$ , whereas at Reducin so small a degree of turbulence could be observed on every eleventh night.

Apart from the estimates of the quality of images, the amplitudes of oscillations of star images were also estimated. The radius of the

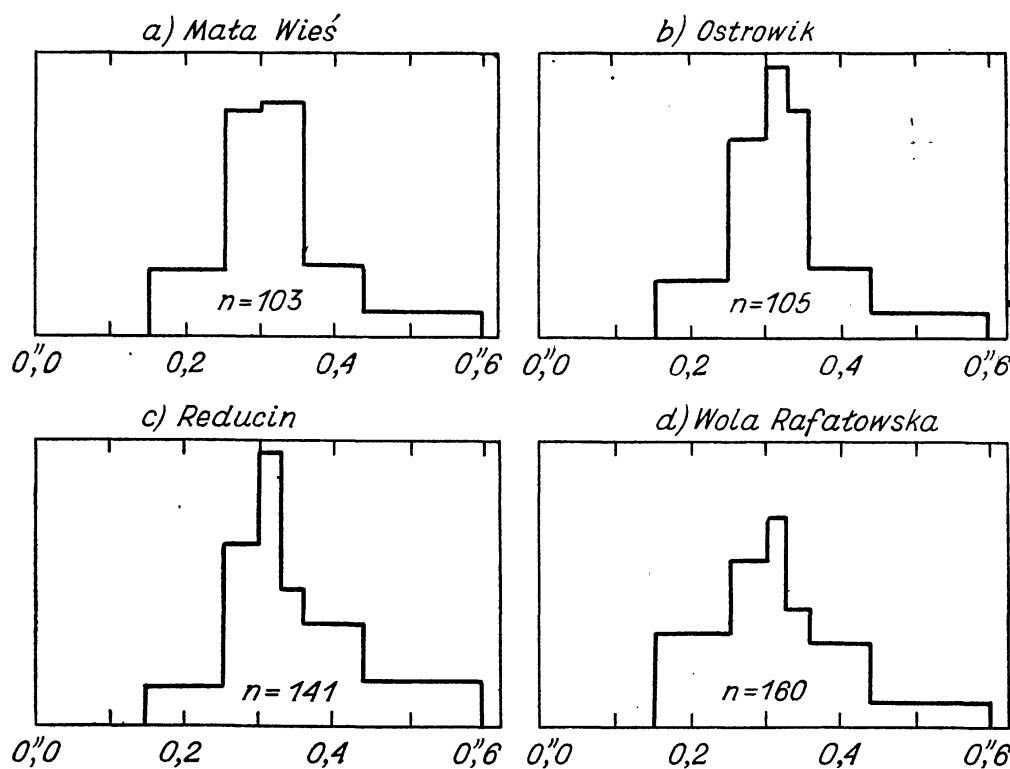


Fig. 1. Histograms of the distribution of atmospheric turbulence at zenith for the particular sites.

first diffraction ring of the star image was taken as a unit of the amplitude of oscillations. The results obtained seem uncertain on account of the large systematic differences between the observers. Thus, for instance, four out of eight observers did not record any observation of oscillations with an amplitude larger than 1, whereas the other four estimated that the oscillations of every fourth star observed exceeded 1. Table 6 shows the percentage frequency of different amplitudes of oscillations of star images: smaller than  $1/2$ , contained between  $1/2$  and 1, and larger than 1, respectively; the systematic differences between observers were eliminated.

Table 6.  
Oscillation of star images (percentage frequency)

Amplitude of oscillations	$\leq 0.5$	0.5 to 1.0	$> 1.0$
Mała Wieś	$51 \pm 4$	$42 \pm 4$	$7 \pm 5$
Ostrowik	$40 \pm 4$	$55 \pm 6$	$5 \pm 5$
Reducin	$53 \pm 4$	$40 \pm 5$	$7 \pm 5$
Wola Rafałowska	$49 \pm 4$	$41 \pm 4$	$10 \pm 5$

The results compiled in Table 6 show that there are no real differences between the sites with regard to the oscillation of star images, perhaps with the exception of the Ostrowik station, where the percentage of observations of low oscillation is smaller than at the other stations.

### Atmospheric extinction

The atmospheric extinction was determined on each clear night. For this purpose, ten stars situated at the height between  $5^{\circ}$  and  $15^{\circ}$  above the horizon were compared visually by the Argelander method with stars situated higher than  $40^{\circ}$  above the horizon. Air mass values used for reducing the results to the zenith were found in the same way as in the case of the observations of turbulence.

Altogether, about 4000 estimates of extinction were made by Argelander's method. The values of extinction at the zenith between  $0^m10$  and  $0^m50$  were obtained for particular nights, whereas the mean error of determining zenith extinction for one night on the basis of ten observations by the Argelander method is about  $\pm 0^m025$ .

The systematic differences between the observers were eliminated in the course of a discussion of observations made at the observers' meetings held at Ostrowik. The mean values of extinction at the zenith for the different sites are given in Table 7.

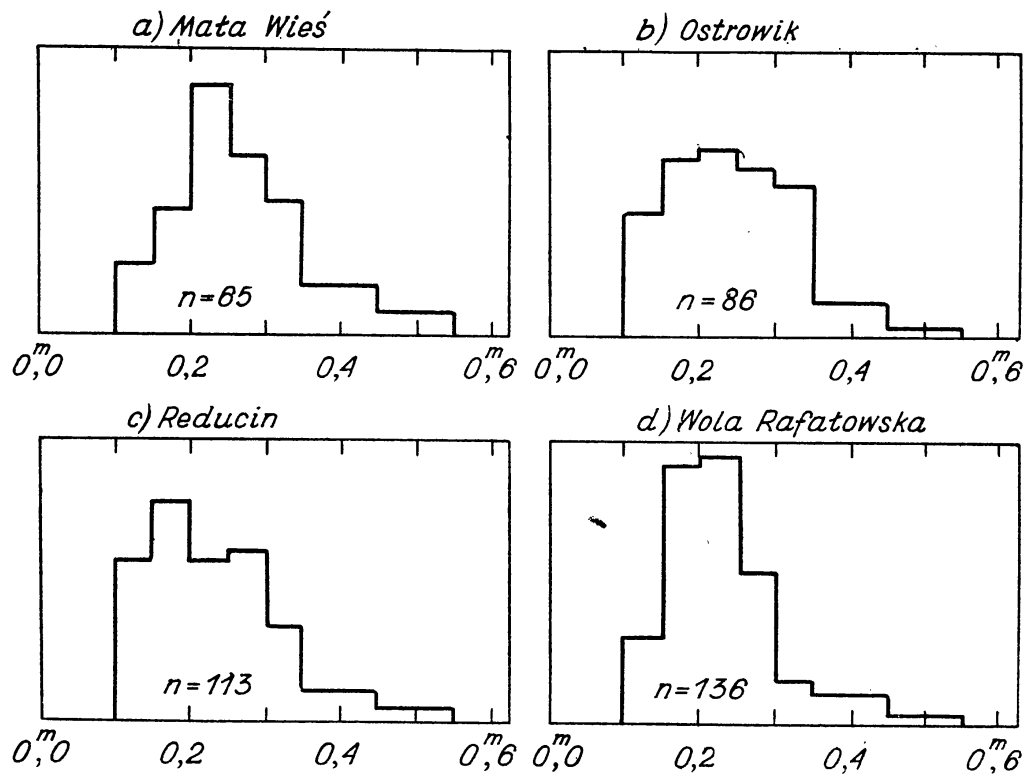


Fig. 2. Histograms of the distribution of extinction at the zenith for the particular sites.

Table 7.  
Extinction at the zenith

Mała Wieś	$0^m 257 \pm 0^m 011$
Ostrowik	$0^m 247 \pm 0^m 010$
Reducin	$0^m 227 \pm 0^m 008$
Wola Rafałowska	$0^m 217 \pm 0^m 006$

Histograms showing the frequency of observed extinction at the zenith for particular sites are shown in Fig. 2.

It can be seen from Figure 2 and from Table 7 that extinction at Wola Rafałowska and Reducin is smaller than at the remaining sites. The site at Wola Rafałowska is also characterized by the smallest fluctuation of extinction from one night to another: the standard deviation of the distribution of extinction at Wola Rafałowska is  $\pm 0^m 07$ , whereas for the other sites it is  $\pm 0^m 09$ . In general, the differences in extinction between different sites are not large.

#### Visual limiting magnitude

Apart from determining extinction, air transparency was also studied by observing the stars in the region of the North celestial Pole. On every night on which the Pole Star was visible, a note was made of the faintest star visible through a small refracting telescope of diameter 45 millimeters and eightfold magnifying power. Beginning on February 25, 1955, observations of limiting magnitude were made with the naked eye to avoid any influence being exerted by systematic differences between the telescopes.

About seven hundred estimates of visual limiting magnitude were made. In the compilation of the observational data, the results of the observations with the telescopes were reduced to terms relating to the observations made with the naked eye. This was done by subtracting a constant  $4^m 0$  from the values observed with the use of telescopes; the constant being the difference between the mean limiting magnitude observed with the use of a telescope and that observed without. The combined data from all the stations and from all the observers formed the basis of averages. The corrections for the systematic errors of the observers were next allowed for, as in the case of the quality of star images. Then the medians of the distribution of limiting magnitude for particular localities were found; they are given in Table 8.

Table 8.  
Visual limiting magnitude (the medians)

Mała Wieś	$5^m 8 \pm 0^m 2$
Ostrowik	$5^m 8 \pm 0^m 1$
Reducin	$5^m 5 \pm 0^m 1$
Wola Rafałowska	$5^m 8 \pm 0^m 1$

It can be seen that the differences between the localities of testing are not large. Only Reducin is characterized by a somewhat smaller limiting magnitude than the remaining stations.

### Visibility of the Milky Way

Measurements of the visibility of the Milky Way were made from May 1 to December 15 each year on moonless nights, when cloudiness was not greater than 2. A visual photometer was used, similar to that of Yntema\*). The diameter of the field of vision was 3°. Chosen regions of the sky were alternately measured: the region in the Milky Way surrounding  $\varphi$  Cyg and a region lying beyond the Milky Way, namely the region around the middle of the arc connecting the stars  $\alpha$  Lyr and  $\chi$  Lyr. Each night a series of twelve measurements were made.

The ratio of the surface brightness of the region situated in the Milky Way to that of the region beyond the Milky Way is denoted by  $k$ . The precision of determination of the ratio  $k$ , computed for one night from twelve observations of the Milky Way and from twelve observations of the region situated beyond it, is about 10 per cent of the value of  $k$ .

The systematic differences between the observers were taken into account in the same way as in the observations of image quality.

Unfortunately the observational material is very small, being only 135 series of measurements for all the four sites.

Table 9 shows the number of nights on which the visibility of the Milky Way was observed at the particular stations, and the mean values of  $k$  together with their mean errors.

Table 9.  
Visibility of the Milky Way

	number of nights	$k$
Mała Wieś	25	$1.61 \pm 0.02$
Ostrowik	30	$1.59 \pm 0.01$
Reducin	41	$1.58 \pm 0.01$
Wola Rafałowska	39	$1.67 \pm 0.03$

We can see that the differences in the visibility of the Milky Way between Mała Wieś, Ostrowik and Reducin are small: only the station at Wola Rafałowska seemed to show slightly better visibility of the Milky Way though the margin of variation of the results is greater here than at the other stations.

The conclusion that the climatological conditions are similar for all the sites seems obvious from the fact that these stations are situated near one another (Mała Wieś and Wola Rafałowska are the furthest apart, at a distance of 82 km) — on a lowland and in a region meteorologically stable.

\*) Yntema. L., *Publ. Astr. Lab. Groningen*, No 22, 1909.

## Influence of meteorological conditions on turbulence, extinction and limiting magnitude

On the basis of the observational data collected, a test was made of the influence of the meteorological conditions (temperature, humidity, wind and cloudiness) on turbulence, extinction and limiting magnitude. It should be stated at the outset that close connections between these factors are not to be expected, because turbulence, extinction, and limiting magnitude are influenced by the conditions in all the layers of the atmosphere, whereas the meteorological observations show the conditions immediately above the Earth's surface.

As an example, Table 10 shows the coefficients of correlation between temperature and extinction (column 2), and humidity and extinction (column 3) for the particular localities.

Table 10.

Coefficients of correlation between extinction and temperature, and between extinction and humidity

	extinction vs temperature	extinction vs humidity
Mała Wieś	+ 0.27	- 0.04
Ostrowik	- 0.02	- 0.12
Reducin	+ 0.18	- 0.28
Wola Rafałowska	- 0.17	- 0.12

So we see that the coefficients of correlation are not large, they vary from station to station, and at different stations they even have a different sign.

This means that extinction, and similarly turbulence and limiting magnitude depend only slightly on the temperature and humidity observed on the Earth's surface.

However, it is possible to detect the dependence of the turbulence on the wind velocity and on cloudiness (Table 11). The increase in wind velocity and cloudiness causes an impairment of the star images.

Table 11.

Coefficients of correlation between wind and turbulence, and between cloudiness and turbulence

	turbulence vs wind velocity	turbulence vs cloudiness
Mała Wieś	+ 0.26	+ 0.29
Ostrowik	+ 0.45	+ 0.31
Reducin	+ 0.38	+ 0.20
Wola Rafałowska	+ 0.39	+ 0.18

Turbulence at the zenith,  $t_o$ , was written as a linear function of wind velocity,  $v$ , and cloudiness,  $C$ :

$$t_o = a + bv + cC. \quad (4)$$

For each site, ten such equations were drawn up, which means that 100 to 160 single estimates were used for every equation. The coefficients  $a$ ,  $b$ , and  $c$  computed by the least squares method are given in Table 12 together with their mean errors for particular localities.

Table 12  
Coefficients of eq. (4)

	$a$	$b$	$c$
Mała Wieś	$0''\cdot16 \pm 0''\cdot06$	$0''\cdot06 \pm 0''\cdot08$	$0''\cdot04 \pm 0''\cdot03$
Ostrowik	$0''\cdot16 \pm 0''\cdot02$	$0''\cdot12 \pm 0''\cdot02$	$0''\cdot02 \pm 0''\cdot01$
Reducin	$0''\cdot09 \pm 0''\cdot06$	$0''\cdot10 \pm 0''\cdot03$	$0''\cdot05 \pm 0''\cdot03$
Wola Rafałowska	$0''\cdot02 \pm 0''\cdot08$	$0''\cdot24 \pm 0''\cdot06$	$0''\cdot02 \pm 0''\cdot03$

Table 12 shows that in spite of large differences between the coefficients  $a$ ,  $b$  and  $c$  for different sites, the influence of wind is greater than that of cloudiness (cf. Mergenthaler, *op. cit.*). Similarly, we can state the influence of wind on limiting magnitude, while the influence of other agents is negligible.

In order to establish the functional dependence between limiting magnitude and wind velocity, ten equations of condition were solved, of the form:  $m_o = a + bv$ , where  $m_o$  is the limiting magnitude observed with the naked eye, and  $v$  — the wind velocity in metres per second. Such equations, making use of the data from all the stations, give  $a = 7^m0 \pm 0^m4$ , and  $b = -1^m2 \pm 0^m3$  (cf. Figure 3).

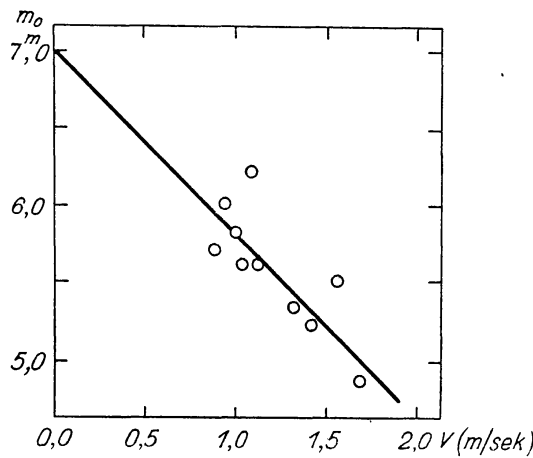


Fig. 3. Dependence between the limiting magnitude and wind velocity.

The influence of wind on the limiting magnitude is explained by the fact that an increase in wind is accompanied by an increase in the amount of dust in the atmosphere. In addition, observations during windy weather are more tiring which can also heighten this effect.

### Correlation of extinction with limiting magnitude and turbulence

Since both limiting magnitude,  $m_0$ , and extinction,  $E$ , are measures of the opacity of the Earth's atmosphere, a relation between these magnitudes is to be expected. Figure 4 shows the dependence of the limiting magnitude on extinction obtained from the data from all the stations.

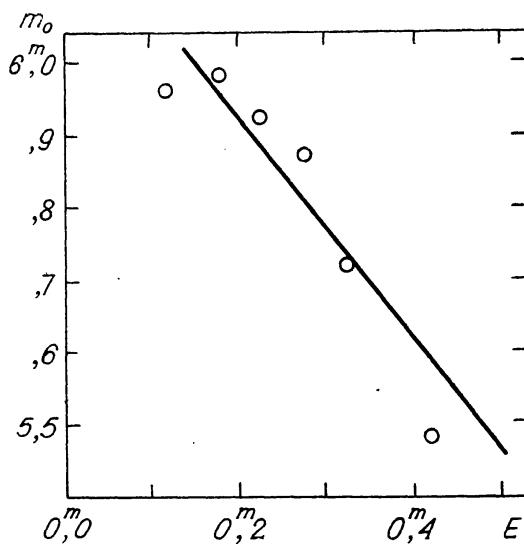


Fig. 4. Dependence between the limiting magnitude and extinction at the zenith.

The regression curve of the form:  $m_0 = a + bE$ , was found by the method of least squares, where  $a = 6^m 23 \pm 0^m 09$ ,  $b = -1.53 \pm 0.35$  and  $m_0$  is the mean limiting magnitude for a given interval of  $E$ .

The relation between limiting magnitude,  $m_0$ , and extinction  $E$  is to be expected in the form  $m_0 = a - E \sec z$ , where  $z$  is the zenith distance of stars used to determine the limiting magnitude. In this case  $z \approx 38^\circ$ , hence  $\sec z \approx 1.27$ ; this value agrees, within the limits of error, with the value  $b$  obtained above.

There is only a slight correlation between extinction and turbulence, the coefficient of correlation being  $\rho = 0.11$ .

### Areas of correlated extinction and areas of correlated turbulence

It is possible to find a relation between magnitudes of extinction on one night in different localities; in general the differences in extinction between the sites situated near one another are smaller than those between more distant localities.

The coefficients of correlation between the simultaneous values of extinction obtained at each pair of observing sites, were computed by means of the equation:

$$\rho = \sqrt{\frac{(E_1 - \bar{E}_1)(E_2 - \bar{E}_2)}{\sigma_{E_1}^2 - \epsilon^2} \sqrt{\frac{\sigma_{E_2}^2}{\sigma_{E_1}^2 - \epsilon^2}}}, \quad (5)$$

where  $E_1$  and  $E_2$  are simultaneous values of extinction at both sites,  $\sigma_{E_1}$  and  $\sigma_{E_2}$  — the standard deviations of the distributions of extinction at these sites, and  $\epsilon$  — the error in determining extinction at each of the sites.

The error  $\epsilon$  was determined on the basis of observations made during a few days' meeting of all observers at the Ostrowik station. The results of simultaneous determinations of an extinction by two observers, placed about twenty metres apart, were put into equation (5). Substituting in the left hand side of this equation  $\rho = 1$ , one could determine the value of errors for each pair of observers. The errors determined in this way were approximately  $\pm 0.025$ .

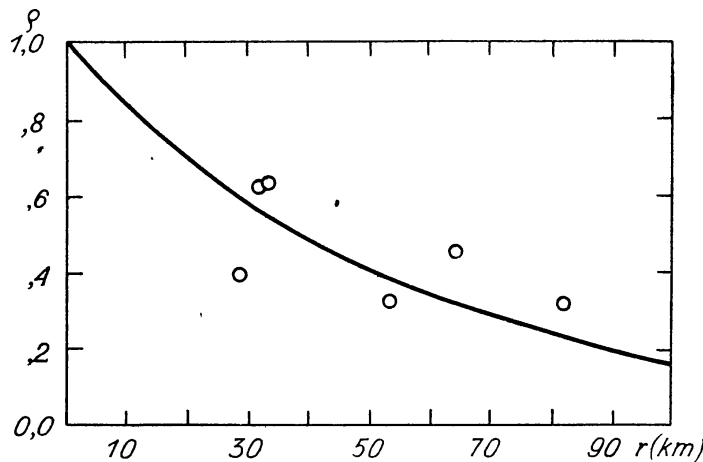


Fig. 5. Coefficients of correlation between the simultaneous values of extinction vs. the distance between the corresponding pair of localities.

Figure 5 gives the coefficients of correlation obtained from formula (5) as a function of the distance between the corresponding pair of localities. Next, the dependence of the coefficient of correlation on the distance was found by the method of least squares. We assumed the dependence of the form  $\rho = \exp(-r/\alpha)$ , where  $r$  is the distance between the corresponding sites. We obtained  $\alpha = 55 \pm 10$  kilometres.

The extent of the areas on which turbulence was correlated, was determined in an analogous way (Fig. 6). The value  $\alpha = 37 \pm 9$  kilometres was obtained.

These results show that the correlation between simultaneous determinations of extinction and that between simultaneous determinations of atmospheric turbulence fall to the value  $1/e$  when the distance between the observing sites is between 35 and 55 kilometres.

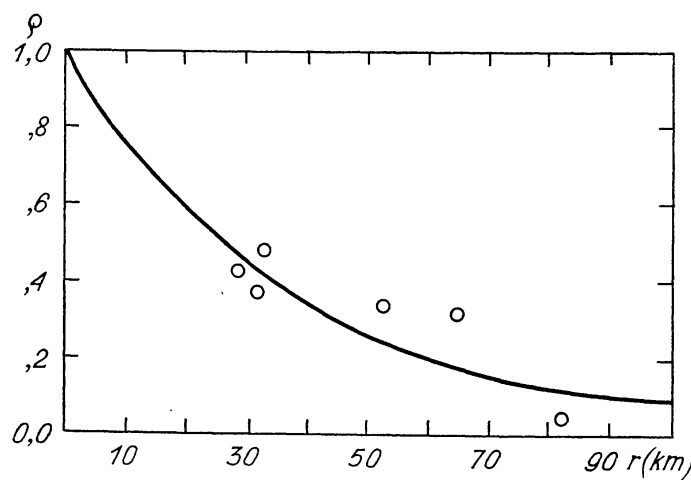


Fig. 6. Coefficients of correlation between the simultaneous values of turbulence vs. the distance between the corresponding pair of localities.

On behalf of the Organizing Committee of the Central Astronomical Observatory of the Polish Academy of Sciences, and on their own account, the authors wish to express their sincere gratitude to Prof. S. L. Piotrowski for his helpful suggestions during the course of the survey. They wish also to thank Mrs T. Stodólkiewicz, Mr J. Hanasz, Mr A. Kruszewski, and Mr. A. Stawikowski who assisted in the compilation of the observation material.

Warsaw, July 1959.

Astronomical Institute  
of the Polish Academy of Sciences  
and  
Warsaw University Observatory.

This investigation was partly supported by the Institute of Geophysics of the Polish Academy of Sciences.

K. Serkowski  
J. Stodólkiewicz

## Performance of the Quartz Clock Z3 of the Latitude Station of the Polish Academy of Sciences in the Year 1958

by

I. Domiński

The first quartz clock of the Latitude Station of the Polish Academy of Sciences at Borowiec was put into operation in August 1957. It was constructed by Stanisław Cierniewski, consulting engineer of the Station. The clock is supplied with a quartz crystal of the Telephones and Cables Ltd, London; it is kept in a double thermostat controlled by mercury contact thermometers. The internal temperature amounts to about 48.5°C. The frequency is demultiplied in the following way:

from 100 kc to 25 kc  
" 25 " 5 "  
" 5 " 1 "

The synchronous motor is fed by an electric current of a frequency of 1 kc. The motor operates mechanical one-second contacts. The symbol of the clock is Z3.

In the initial stage the clock very soon changed its rate. It is only in December 1957 that the rate became stabilized and adopted a linear character: the drift remained more or less stable amounting to +0.286 ms/d<sup>2</sup>. For unknown reasons there occurred in August 1958 a change in the drift which may have possibly been due to a rather severe shock.

The first thing in working out the rate of the clock was to remove the provisional parabolic component expressed by the formula:

$$\text{Red} = -20.530 - 1.82499(t - t_0) - 0.0001430(t - t_0)^2$$
$$t_0 = 1958. \text{VIII. } 21.0 \text{ U. T.}$$

valid until August 21, 1958 and from then on by

$$\text{Red} = -20.530 - 1.82632(t - t_0) - 0.0001696(t - t_0)^2$$
$$t_0 = 1958. \text{VIII. } 21.0 \text{ U. T.}$$

The reduction was made according to the formula:  $\Delta Z3 + \text{Red} = \Delta' Z3$  where  $\Delta Z3$  denotes the true correction of the clock and  $\Delta' Z3$  — the correction of the fictitious clock. I applied these latter corrections in the further course of my work.

The clock Z3 was regularly compared with the time signals GBZ, FYP, ROR and DAN transmitted on long waves and with time obser-

vations on two transit instruments. Even cursory observations showed that the signals GBZ were encumbered with smaller errors than the other signals. Therefore, in working out the clock's rate I took mainly account of the GBZ signals, except in November and December 1958, when they ceased to be transmitted, I made use of the FYP and ROR signals. The clock-corrections obtained from time-signals were converted into the system TU<sub>2</sub> on base of data of the Soviet Time Service published in „Etalonnoje Vremia“.

The results are presented in graphic form in Fig. 1 where also clock-corrections obtained by smoothing the observations, are given. Fig. 2 contains a diagram of the frequency of the 100 kc generator of clock Z3.

The above mentioned material served for determining the long-term stability of the clock and for comparing it with other clocks.

The quality of a clock may be defined by the method of H. Smith of the Greenwich Observatory [1]. This method consists in determining the mean of the absolute values of the second differ-

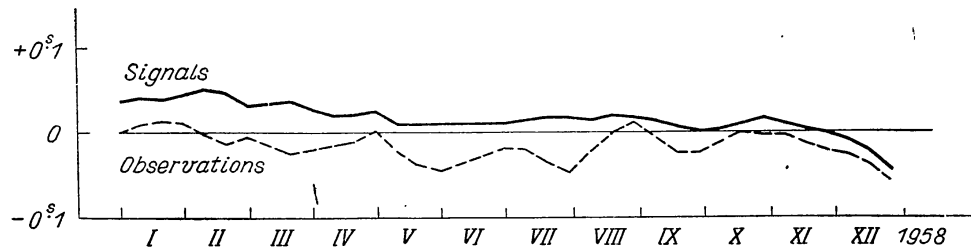


Fig. 1. Corrections of clock Z3 in the system TU<sub>2</sub>. The parabolic component has been eliminated. The corrections obtained from „Etalonnoje Vremia“ are represented by the full line, those obtained from smoothed observations also on the basis of TU<sub>2</sub> — by the dotted line.

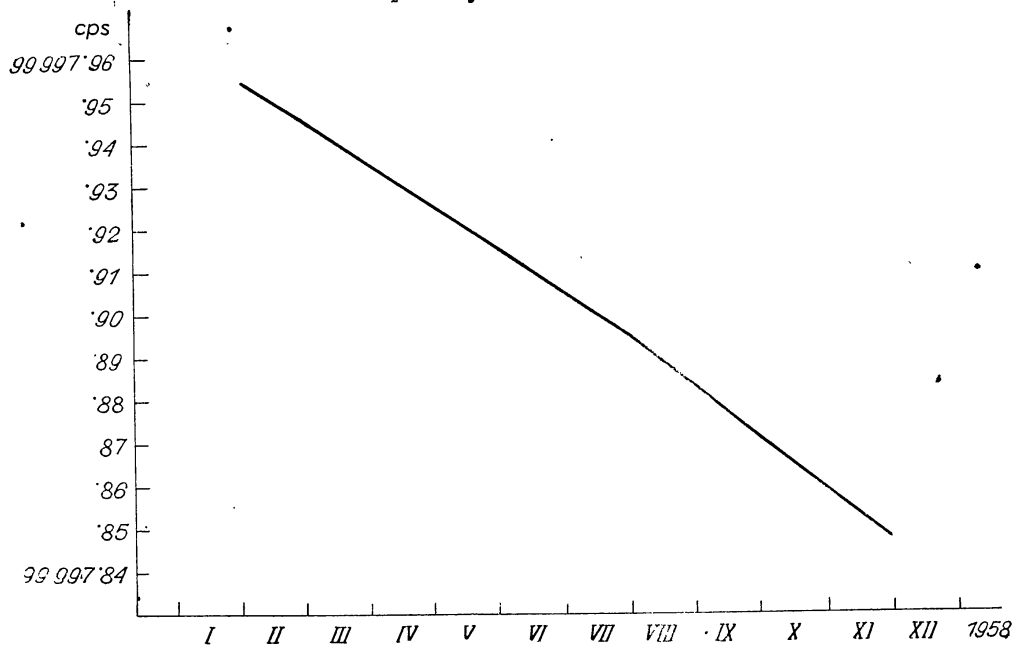


Fig. 2. Frequency of the 100 kc generator of clock Z3.

ences of a clock's rate. To this end a table is set up showing the mean daily runs in particular months and the respective differences within two years. The rate of the clock should be determined with respect to a good standard independent of irregularities in the rate of the rotation of the Earth. The only standard of that kind at present available to me were the results published in „Etalonnoje Vremia“. In order to determine the value of a clock and its long-term stability a period of two years was chosen. However, one year should yield sufficiently good results for evaluating a clock's quality.

Table I

1958	$\Delta' Z_3$	M	D	e	E
I	+ 0.0386				
II	458	+ 0.00024	- 0.00072	- 0.00090	- 0.00060
III	315	- 48	+ 18	- 23	+ 30
IV	225	- 30	- 15	+ 43	- 3
V	118	- 35	+ 28	- 1	+ 40
VI	95	- 7	+ 27	- 45	+ 39
VII	155	+ 20	- 18	- 13	- 6
VIII	162	+ 2	- 31	+ 62	- 19
IX	74	- 29	+ 31	- 46	+ 43
X	79	+ 2	- 15	- 63	- 3
XI	+ 39	- 13	- 78	-	66
XII	- 239	- 91			

$\Delta' Z_3$  — correction of the fictitious clock, monthly mean

M — daily rate in sec/day, monthly mean

D — change of rate in sec/day/month

e — second difference of the rate in sec/day/month<sup>2</sup>

E — deviation of the clock's drift from its mean value,

$$E = D_i - D_{\text{mean}}$$

A simple calculation yields:

$$|e|_{\text{mean}} = 0.00043 \text{ sec/day/month}^2$$

Another criterion for evaluating the quality of a clock has been suggested by E. Guyot [2]. According to him a measure of the quality of a clock is the mean of the absolute values of deflections in the drift, denoted by E. For Z3:

$$|E|_{\text{mean}} = 0.00031 \text{ sec/day/month.}$$

For comparing Z3 with other clocks I am adding a table taken from papers [¹] and [²].

Table 2.

Clock		$ e _{\pi}$	$ E _{\pi}$
E5, Abinger	R	0.00008	0.00007
9A, Dollis Hill	R	0.00006	0.00005
9C, "	R	0.00007	0.00007
EA, "	R	0.00008	0.00008
EB, "	R	0.00017	0.00025
Q 13, NPL	R	0.00015	0.00034
F 1	P	0.00053	-
U, BIH	?	0.00079	0.00050
44 Shortt, BIH	-	0.00131	0.00076
1395 Leroy, "	-	0.00531	0.00321
Z3, Borowiec	P	0.00043	0.00031

P = quartz ring

R = quartz plate

As may be seen from the above Table, Z3 is not a bad clock. Distinctly superior to it are only English clocks with quartz rings. The results obtained with the Z3 clock may be regarded as very good considering that the performance of the clock was impaired by rather frequent disturbances and short interruptions which were eliminated only in the second half of the year 1958.

#### REFERENCES:

- [¹] Humphry M. Smith, Quartz Clocks of the Greenwich Time Service, *Monthly Notices* **113**, 67–80, 1952.
- [²] Edmond Guyot, Comment Evaluer la Précision d'une Horloge, *Annales Françaises de Chronométrie*, 2<sup>me</sup> Sér. tome **XII**, 28 Année 3 trim.

Latitude Station of the Polish Academy of Sciences  
Borowiec, July 20, 1959.

I. Domiński.

---

M. Kamiński: Approaches of Comet P/Wolf I to Jupiter. — J. Smak: Population II Stars. Part 1. Homogeneous Stellar Models with Convective Envelopes. Part 2. Semi-theoretical (B – V) — T. Relation for the Subdwarfs. — A Michałowska and J. Smak: A Study of the Kinematical Properties of High Velocity Stars. — K. Serkowski and J. Stodółkiewicz: A Study of the Microclimate in the Region South and East of Warsaw. — I. Domiński: Performance of the Quartz Clock Z3 of the Latitude Station of the Polish Academy of Sciences in the Year 1958.

---

Adresse de la Rédaction: Cracovie, Pologne, rue Copernic 27

Państwowe Wydawnictwo Naukowe — Kraków 1960

Nakład 596 + 124. Ark. wyd. 5½. Ark. druk. 4¾ Pap. ilustr. III kl., 100 gr. 70 x 100. Podpisano do druku 14. XI. 1960. Druk ukończono w listopadzie 1960. Zamówienie Nr 3106, 28. VI. 1960.

Drukarnia Związkowa — Kraków, ul. Mikołajska 13

**Cena zł 20.-****Contenu du fascicule (Vol. 10, 3, 1960):**

<b>M. Kamiński:</b>	Approaches of Comet P/Wolf I to Jupiter . . . . .	p. 139
<b>J. Smak:</b>	Population II Stars. Part 1: Homogeneous Stellar Models with Convective Envelopes . . . . .	" 153
	Part 2: Semi-theoretical $B(-V) - T_e$ Relation for the Subdwarfs . . . . .	" 167
<b>A. Michałowska and J. Smak:</b>	A Study of the Kinematical Properties of High Velocity Stars . . . . .	" 179
<b>K. Serkowski and J. Stodółkiewicz:</b>	A Study of the Micro-climate in the Region South and East of Warsaw . . . . .	" 189
<b>I. Domiński:</b>	Performances of the Quartz Clock Z3 of the Latitude Station of the Polish Academy of Sciences in the Year 1958 . . . . .	" 205

POLSKA AKADEMIA NAUK  
KOMITET ASTRONOMII

---

ACTA  
ASTRONOMICA

VOL. 10

4

WARSZAWA — 1960 — KRAKÓW

ACADEMIE POLONAISE DES SCIENCES  
Comité d'Astronomie

ACTA  
ASTRONOMICA

JOURNAL INTERNATIONAL

fondé par

TH. BANACHIEWICZ

Vol. 10

1960

CRACOVIE — VARSOVIE

## Table des articles

Vol. 10.

A. G. Pacholczyk and J. Stodółkiewicz	On the Gravitational Instability of Some Magnetohydrodynamical Systems of Astrophysical Interest . . . . .	1
T. Jarzębowski	Relation between Light-variation and Magnetic Variation in Magnetic Alpha Variables . . . . .	31
E. Rybka	On Systematic Differences in the Harvard Photometries . . . . .	53
R. Szafraniec	Minima of Eclipsing Variables observed in 1959 . . . . .	69
T. Jastrzębski	Orbite de ADS 15270 AB = $\Sigma$ 2822 = $\mu$ Cyg . . . . .	71
M. Kamiński	Note to the Editor . . . . .	74
F. Kępiński	Researches on the Motion of Comet P/Wolf I (Part XVIII: Disturbed Motion of the Comet in 1959) . . . . .	75
W. Zonn	Critérium de l'identité de deux comètes . . . . .	85
R. Szafraniec	Photographic Observations of CE Cassiopeiae . . . . .	89
T. Jarzębowski	The Light-curves of Eclipsing Binaries . . . . .	99
J. Dobrzycki	Light Curve of Magnetic Star HD 215441 . . . . .	119
S. Nowak	Latitude Variations of Borowiec in the Period 1957.8—1960.1 . . . . .	123
M. Kamiński	Corrections of Right Ascensions of Planets in 1959 from Transit Observations . . . . .	135
J. Smak	Approaches of Comet P/Wolf I to Jupiter on the Background of Centuries . . . . .	139
	Population II Stars. Part 1: Homogeneous Stellar Models with Convective Envelopes . . . . .	153
	Part 2: Semi-theoretical $(B - V) - T_e$ Relation for the Subdwarfs . . . . .	167
A. Michałowska and J. Smak	A Study of the Kinematical Properties of High Velocity Stars . . . . .	179
K. Serkowski and J. Stodółkiewicz	A Study of the Micro-climate in the Region South and East of Warsaw . . . . .	189
I. Domiński	Performances of the Quartz Clock Z <sub>3</sub> of the Latitude Station of the Polish Academy of Sciences in the Year 1958 . . . . .	205
F. Kępiński	The Motion of P/Comet 1906 IV (Kopff) in the Sphere of Predominance of Jupiter in the first half of the Year 1954 . . . . .	209
M. Kamiński	Comet P/Wolf I in 1958 . . . . .	221
K. Serkowski	Photographic Measurements of Polarization in the Region of the Association III Cephei . . . . .	227

**Vol. 10****A. A.**

<b>T. Jarzębowski</b>	Photoelectric Observations of Magnetic Stars . . . . .	237
<b>O. Czyżewski</b>	810 MHz Radio Bursts in Correlation with Chromospheric Flares . . . . .	247
<b>T. Jastrzębski</b>	Éléments orbitaux de ADS 15988 = $\Sigma$ 2912 = 37 Peg	257
<b>B. Morkowska</b>	Precise Astrographic Positions of Minor Planets Obtained at the Poznań University Observatory	263
Liste alphabétique de noms . . . . .		273
Table des matières . . . . .		276

# ACTA ASTRONOMICA

Vol. 10, 4.

1960

## The Motion of P/Comet 1906 IV (Kopff) in the Sphere of Predominance of Jupiter in the first half of the Year 1954

by

F. Kępiński

In my recent paper, *Acta Astronomica*, Vol. 8, fasc. 4 (1958) I considered the motion of the above mentioned Comet in the period 1951—1958 taking into consideration the perturbations of the 6 great planets (Jupiter, Saturn, the Earth, Venus, Mars and Uranus) in the heliocentric system of coordinates.

However, I had to pass to equatorial coordinates already in the course of my first computation for the following reasons:

The Comet made a very close approach to Jupiter up to a distance of 0.17 a. u. on 30th March 1954. The perturbations caused by Jupiter were very great, chiefly in the elements determining the position of the plane of the Comet's orbit, i. e. the longitude of the node  $\Omega$  and the inclination of the orbital plane to the ecliptic  $i$ . It was thus necessary to realize a more quiet run of these or other elements. Moreover, I was compelled to reduce the intervals of mechanic quadrature to  $2\frac{1}{2}$  days but this appeared to be still insufficient for an accurate computation.

Thus, after the rediscovery of the Comet by Miss Dr E. Roemer at the Flagstaff Station of the U. S. Naval Observatory (Arizona) on the 25th June 1958, I thought it necessary to repeat my computations for the critical period of 1954 by diminishing the intervals of integration to 1.25 day for the Comet's motion in heliocentric coordinates and taking them throughout as equal to 5 days in the jovicentric ones.

Taking up this work I had in mind to confirm practically the theoretical evidence: the movements of comets or small planets in the period of their close approach to a great planet can be explored most accurately by relating them to this planet (planetocentric, jovicentric system); nevertheless in some cases it is advisable to control planetocentric computations by heliocentric ones. This in view, both methods had to be fitted to one another by appropriately adjusting the intervals of integration and, of course, by taking into consideration the same celestial bodies, if both methods were to lead to the same result.

My first computation established in the heliocentric system is contained in the above quoted paper which is of no special importance for the present investigation; but I want to mention that it differed from the second heliocentric computation (accomplished in

narrower intervals) by small oscillations of rather insignificant influence on my further work.

The subject of the present paper is a comparison of the results of both methods applied to the Comet 1906 IV during the critical period of 1954. In order to attain this purpose, a high degree of accuracy was preserved. Therefore it would be of importance to make known and at the same time to recommend the procedure and the formulas to be used in practice.

Taking into account that the heliocentric coordinates of great planets (Coordinates of the five outer planets *Astr. Papers of the Amer. Eph. a. Naut. Alm.*, Vol. XII, Washington, 1951) are referred to the terrestrial equator and not to the ecliptic, it was preferable from the very beginning to relate the heliocentric as well as the planetocentric elements to the Earth's equator. This transformation can be made by means of the known formulae [¹].

### §. I. The transformation of heliocentric into jovicentric elements of the Comet's orbit. Disturbing bodies: Jupiter, Saturn, the Earth, Venus, Mars, Uranus...

With a view to study the Comet's jovicentric motion during its sojourn in Jupiter's predominance sphere, we had to start from the heliocentric coordinates of both bodies. These coordinates were known from the preceding period when the bodies were still at a considerable distance one from another.

Let . . . .  $t_0 - 2w, t_0 - w, t_0, t_0 + w, t_0 + 2w, \dots$  be the equidistant epochs of the preceding heliocentric computation for which the perturbations of the Comet's orbital elements produced by the 6 great planets as well as the corresponding systems of elements were calculated. The epoch  $t_0$  was accepted as a new epoch of the jovicentric motion of the Comet. The derivatives of the heliocentric coordinates of Jupiter with respect to time could be formed by interpolation, but those of the Comet, on the contrary, might be taken from its disturbed heliocentric elements for the epoch  $t_0$  throughout as results from the following formulae [²].

#### Denotations and formulae.

$x, y, z; x', y', z'$  — heliocentric equatorial coordinates of the Comet and their derivatives  
 $x_1, y_1, z_1; x'_1, y'_1, z'_1$  — heliocentric equatorial coordinates of Jupiter (Saturn,...) and their derivatives,

$$r = \sqrt{x^2 + y^2 + z^2} \text{ — heliocentric radius vector of the Comet}$$

$$r_1 = \sqrt{x_1^2 + y_1^2 + z_1^2} \text{ — heliocentric radius vector of Jupiter.}$$

$$\begin{aligned} x &= a_1 r & x' &= a_1 r' + b_1 r v' & r' &= \frac{dr}{dt} = \frac{k}{\sqrt{p}} e \sin v \\ y &= a_2 r & y' &= a_2 r' + b_2 r v' \\ z &= a_3 r & z' &= a_3 r' + b_3 r v' & r v' &= r \frac{dv}{dt} = \frac{k \sqrt{p}}{r} \end{aligned}$$

$$\begin{Bmatrix} a_1 \\ b_1 \\ a_2 \\ b_2 \end{Bmatrix} = \begin{Bmatrix} \cos \Omega \\ \sin \Omega \cdot \cos i \\ \sin \Omega \\ \cos \Omega \cdot \cos i \end{Bmatrix} = \begin{Bmatrix} \cos u & -\sin u & 0 & 0 \\ -\sin u & -\cos u & 0 & 0 \\ 0 & 0 & \cos u & -\sin u \\ 0 & 0 & \sin u & \cos u \end{Bmatrix}$$

$$\begin{Bmatrix} a_3 \\ b_3 \end{Bmatrix} = \{\sin i\} \cdot \{\sin u \cos u\}$$

## I. a The heliocentric motion of the Comet (ellipse)

 $a$  — semi-major axis $e = \sin \varphi$  eccentricity $M$  — mean anomaly $i$  — inclination of the Comet's orbit on equator $\Omega$  — longitude of the ascending node $\omega$  — longitude of the perihelion

} 1950.0

$\mu = k' : a^{\frac{3}{2}}$        $k'' = 3548'' \cdot 187607$        $p = a(1 - e^2) = a \cdot \cos^2 \varphi$

$r \cdot \sin v = a \cdot \cos \varphi \cdot \sin E,$        $r = a(1 - e \cos E) = p : (1 + e \cos v)$

$r \cdot \cos v = a(\cos E - e),$        $\operatorname{tg} \frac{1}{2}v = \operatorname{tg}(45^\circ + \frac{1}{2}\varphi) \cdot \operatorname{tg} \frac{1}{2}E$

 $u = \omega + v$  orb. long. of the Comet

$$E - e \sin E = M = \mu(t - T), \quad E \text{ — eccentric anomaly,}$$
 $v \text{ — true anomaly,}$ 
 $T \text{ — perihelion time.}$

## I. b The jovicentric motion of the Comet (hyperbola). Some denotations are maintained for the sake of brevity

 $a$  — semi-major axis $e$  — sec  $\psi$  $N$  — mean anomaly $i$  — inclination of the Comet's orbit to the eq. $\Omega$  — longitude of the ascending node $\tilde{\omega}$  — longitude of the perijovium

} 1950.0

$\mu'' = \operatorname{Mod.} \sqrt{m_1 \cdot k'} : a^{\frac{3}{2}}, \quad p = a(e^2 - 1), \quad a = -a$

$r \cdot \sin v = a \cdot \operatorname{tg} \psi \cdot \operatorname{tg} F, \quad r = a(e \sec F - 1) = p \cdot \cos \psi : (\cos \psi + \cos v)$

$r \cdot \cos v = a(e - \sec F), \quad \operatorname{tg} \frac{1}{2}v = \operatorname{ctg} \frac{1}{2}\psi \cdot \operatorname{tg} \frac{1}{2}F, \quad m_1 = 0.000954786104$

$\operatorname{Mod.} e \cdot \operatorname{tg} F - \log \operatorname{tg}(45^\circ + \frac{1}{2}F) = \mu \cdot (t - T) = N$

 $F$  ecc. anomaly,       $v$  true anomaly,       $T$  perijovium time

$\operatorname{Mod. log. nat.} = 0.4342944819$

## I. c Denotations and formulas for the transformation of heliocentric into jovicentric motion of the Comet.

$\xi = x - x_1$

$\xi' = x' - x'_1$

$\eta = y - y_1$

$\eta' = y' - y'_1$

$\zeta = z - z_1$

$\zeta' = z' - z'_1$

$\rho = \sqrt{\xi^2 + \eta^2 + \zeta^2}$

radius vector of Com. from Jupiter

$$\begin{aligned} k\sqrt{m_1} \cdot \sqrt{p} \cdot \sin i \cdot \sin \Omega &= \eta\zeta' - \zeta\eta' = \Delta_\xi \\ -k\sqrt{m_1} \cdot \sqrt{p} \cdot \sin i \cdot \cos \Omega &= \xi\xi' - \xi'\xi = \Delta_\eta \quad k\sqrt{m_1} = 0.000531538207 \\ k\sqrt{m_1} \cdot \sqrt{p} \cdot \cos i &= \xi\eta' - \eta\xi' = \Delta_\zeta \quad \text{Mod. } k''\sqrt{m_1} = 47''61501558 \end{aligned}$$

$$\begin{aligned} k\sqrt{m_1}\sqrt{p} \cdot \sin i &= \sqrt{\Delta_\xi^2 + \Delta_\eta^2}, \quad k\sqrt{m_1}\sqrt{p} = \sqrt{\Delta_\xi^2 + \Delta_\eta^2 + \Delta_\zeta^2} \\ \operatorname{tg} i &= \sqrt{\Delta_\xi^2 + \Delta_\eta^2} : \Delta_\zeta, \quad \operatorname{tg} \Omega = -\Delta_\xi : \Delta_\eta \end{aligned}$$

whence:  $p, \Omega, i$ .

$$V_h^2 = \xi'^2 + \eta'^2 + \zeta'^2 = k^2 m_1 \left( \frac{2}{\rho} - \frac{1}{a} \right)$$

$$a = \frac{\rho : 2}{1 - (V_h^2 : k^2 m_1) \cdot (\rho : 2)} \quad \mu'' = \frac{\text{Mod. } k''\sqrt{m_1}}{a^{3/2}}$$

whence:  $a, \mu''$ .

$$\begin{aligned} e. \sin v &= (\sqrt{p} : k\sqrt{m_1} \rho) \cdot (\xi\xi' + \eta\eta' + \zeta\zeta') \\ e. \cos v &= (p : \rho) - 1 \end{aligned}$$

whence:  $e, v$ .

$$\begin{aligned} \rho. \sin u &= \zeta \sqrt{\Delta_\xi^2 + \Delta_\eta^2 + \Delta_\zeta^2} : \sqrt{\Delta_\xi^2 + \Delta_\eta^2} \\ \rho. \cos u &= (\eta \cdot \Delta_\xi - \xi \cdot \Delta_\eta) : \sqrt{\Delta_\xi^2 + \Delta_\eta^2} \end{aligned}$$

whence:  $\rho, u, \omega = u - v, \tilde{\omega} = \omega + \Omega$ .

$$\text{Mod. } e. \operatorname{tg} F - \log \operatorname{tg} (45^\circ + \frac{1}{2}F) = \mu(t - T) = N$$

whence:  $F, N, T$ .

## § 2. The computation of the perturbations of the Comet's orbital elements in the jovicentric system.

The disturbing bodies: the Sun, Saturn,....

After having transformed the perturbed heliocentric elements of the Comet's orbit into jovicentric ones for the epochs: ....  $t_0 - 2w$ ,  $t_0 - w$ ,  $t_0$ ,  $t_0 + w$ ,  $t_0 + 2w$ ,.... the computations of the perturbations of jovicentric elements of the Comet were carried out:  $i, \Omega, \tilde{\omega}, e, N, \mu$  in intervals of 5 days and with continuous alteration of these elements, produced by the disturbing bodies (the Sun, Saturn,...) according to the following denotations and formulas.

$\xi, \eta, \zeta$  the jovic. equat. coord. of the Comet and their derivatives  
 $\xi_1, \eta_1, \zeta_1$  the jovic. equat. coord. of the disturbing body (the Sun, Saturn,...) and their derivatives.

$\rho$  jovicentric radius vector of the Comet  $= \sqrt{\xi^2 + \eta^2 + \zeta^2}$

$\rho_1$  jovicentric radius vector of the disturbing body  $= \sqrt{\xi_1^2 + \eta_1^2 + \zeta_1^2}$

$$\begin{Bmatrix} \xi_1 \\ \eta_1 \\ \zeta_1 \end{Bmatrix} = \begin{Bmatrix} -x_1 \\ -y_1 \\ -z_1 \end{Bmatrix} \cdot \begin{Bmatrix} a_1 & b_1 & c_1 \\ a_2 & b_2 & c_2 \\ a_3 & b_3 & c_3 \end{Bmatrix}$$

The structure of the direction coefficients  $a_i, b_i, c_i$ , which here occur, is the same as that of analogous coefficients met in Chapter I, provided that the orbital elements  $i, \Omega, \tilde{\omega}$  as well as the elements  $a, \mu, e$ , and the quantities  $p, v, u, F$  which appear later are understood here as jovicentric ones according to section I. b.

The differentials of perturbations of the hyperbolic orbital elements of the Comet could be obtained then by virtue of the following formulae and denotations.

$$\begin{aligned} w \frac{di}{dt} &= i_w \cdot W & w \frac{de}{dt} &= e_s \cdot S + e_t \cdot T \\ w \frac{d\Omega}{dt} &= \Omega_w \cdot W & w \frac{dN}{dt} &= N_s \cdot S + N_t \cdot T \\ w \frac{d\tilde{\omega}}{dt} &= \tilde{\omega}_s \cdot S + \tilde{\omega}_t \cdot T + \tilde{\omega}_w \cdot W & w^2 \frac{d^2 \mu}{dt^2} &= \mu_s \cdot S + \mu_t \cdot T \end{aligned}$$

$$\begin{aligned} i_w &= (\rho : p) \cdot \cos u & \tilde{\omega}_s &= -\cos v : e \\ \Omega_w &= (\rho : p) \cdot \sin u \cdot \operatorname{cosec} i & \tilde{\omega}_t &= [\sin v + (\operatorname{tg} F : \sqrt{e^2 - 1})] : e \\ e_s &= \sin v, \quad e_t = \cos v + \sec F & \tilde{\omega}_w &= (\rho : p) \cdot \sin u \cdot \operatorname{tg} \frac{1}{2} i \end{aligned}$$

$$N_s = \operatorname{Mod.} \sqrt{e^2 - 1} \cdot [(2\rho : p) - (\cos v : e)] \quad \mu_s = 3a\mu \cdot w \cdot (e : p) \cdot \sin v$$

$$N_t = \operatorname{Mod.} (\sqrt{e^2 - 1} : e) \cdot [1 + (\rho : p)] \quad \mu_t = 3a\mu \cdot w : \rho$$

As for the components of the disturbing function:  $S, T, W$  it is necessary now to take into consideration each disturbing body separately.

### 2.a The disturbing body: the Sun (mass 1).

The components of the disturbing function can be presented as follows.

$$S = \frac{k'' \cdot w}{\sqrt{m_1}} \cdot \sqrt{p} \cdot \left( K \cdot \xi_1 - \frac{\rho}{r_d^3} \right), \quad \xi_1 = -x \text{ jovic. coord. of the Sun } \xi_1, \eta_1, \zeta_1$$

$$T = \frac{k'' \cdot w}{\sqrt{m_1}} \cdot \sqrt{p} \cdot K \cdot \eta_1 \quad \eta_1 = -y_j \quad \rho_1^2 = \xi_1^2 + \eta_1^2 + \zeta_1^2$$

$$W = \frac{k'' \cdot w}{\sqrt{m_1}} \cdot \sqrt{p} \cdot K \cdot \zeta_1 \quad \zeta_1 = -z_j \quad r_d \text{ distance of the Comet from the Sun}$$

$$K = \frac{1}{r_d^3} - \frac{1}{\rho_1^3}, \quad r_d^2 = \rho_1^2 + \rho^2 - 2\rho \cdot \xi_1$$

### 2.b The disturbing body: Saturn (mass $m_s = 0.000285583733$ )

$$S = m_s \cdot \frac{k'' \cdot w}{\sqrt{m_1}} \cdot \sqrt{p} \cdot \left( K \cdot \xi_1 - \frac{\rho}{r_d^3} \right), \quad \xi_1 = x_s - x_i \quad \text{jovic. coord. of Saturn } \xi_1, \eta_1, \zeta_1$$

$$T = m_s \cdot \frac{k'' \cdot w}{\sqrt{m_1}} \cdot \sqrt{p} \cdot K \cdot \eta_1 \quad \eta_1 = y_s - y_i \quad \rho_1^2 = \xi_1^2 + \eta_1^2 + \zeta_1^2$$

$$W = m_s \cdot \frac{k'' \cdot w}{\sqrt{m_1}} \cdot \sqrt{p} \cdot K \cdot \zeta_1 \quad \zeta_1 = z_s - z_i \quad r_d \text{ distance of the Comet from Saturn}$$

$$K = \frac{I}{r_d^3} - \frac{I}{\rho_1^3}, \quad r_d^2 = \rho_1^2 + \rho^2 - 2\rho \cdot \xi_1$$

Special attention is to be paid to the forming of the variation

$$N = N - N_0 = \mu_0 (t - t_0) + w \int \frac{dN}{dt} dt + w^2 \int \int \frac{d\mu}{dt} dt^2 \quad [2]$$

where  $\mu_0$  relatively  $N_0$  denote the initial values of the mean motion and mean anomaly of the Comet corresponding to the epoch  $t_0$ .

The mechanical integration of the above equations is to be carried out for the entire time of sojourn of the Comet in the sphere of Jupiter's predominance. In this manner the Comet's disturbed jovicentric orbital elements can be obtained for the time of the departure of the Comet from the critical sphere. The next step was to transform them again into heliocentric elements admitting the last epochs of the jovicentric calculus as initial of the further heliocentric one.

### §. 3. The transformation of the Comet's jovicentric elements into heliocentric ones.

Referring to the formulae of section I.a for the coefficients  $a_1, b_1$ , wherein the heliocentric elements of the Comet are now to be transformed into jovicentric ones, we calculate first

$$\begin{aligned} \xi &= a_1 \rho & \xi' &= a_1 \rho' + b_1 \rho v' & \rho' &= (k \sqrt{m_1} : \sqrt{p}) e \cdot \sin v \\ \eta &= a_2 \rho & \eta' &= a_2 \rho' + b_2 \rho v' & & \\ \zeta &= a_3 \rho & \zeta' &= a_3 \rho' + b_3 \rho v' & \rho v' &= (k \sqrt{m_1} : \sqrt{p}) : \rho \end{aligned}$$

and then using again the American Tables we obtain by interpolation the heliocentric coordinates of Jupiter  $x_1, y_1, z_1$  and their derivatives  $x'_1, y'_1, z'_1$  for a suitable epoch.

A further computation of the heliocentric elements of the Comet on the basis of the obtained jovicentric ones is performed according to the following formulae.

$$\begin{aligned} x &= x_1 + \xi, & x' &= x'_1 + \xi' \\ y &= y_1 + \eta, & y' &= y'_1 + \eta' \\ z &= z_1 + \zeta, & z' &= z'_1 + \zeta' \end{aligned}$$

$$\begin{aligned} k \sqrt{p} \cdot \sin i \cdot \sin \Omega &= yz' - zy' = D_x \\ -k \sqrt{p} \cdot \sin i \cdot \cos \Omega &= zx' - xz' = D_y \\ k \sqrt{p} \cdot \cos i &= xy' - yx' = D_z \end{aligned}$$

$$k\sqrt{p} \cdot \sin i = \sqrt{D_x^2 + D_y^2}, \quad k\sqrt{p} = \sqrt{D_x^2 + D_y^2 + D_z^2}$$

$$\operatorname{tg} i = \sqrt{D_x^2 + D_y^2} : D_z, \quad \operatorname{tg} \Omega = -D_x : D_y$$

Hence:  $p$ ,  $\Omega$ ,  $i$

$$V_e^2 = x'^2 + y'^2 + z'^2 = k^2 \left( \frac{2}{r} - \frac{1}{a} \right)$$

$$a = \frac{r:2}{1 - (V_e^2: k^2) \cdot (r:2)} \quad \mu'' = k'' \cdot a^{3/2}$$

Hence:  $a$ ,  $\mu''$ .

$$e \cdot \sin v = [\sqrt{p}:(k \cdot r)] \cdot (xx' + yy' + zz')$$

$$e \cdot \cos v = (p:r) - 1$$

Hence:  $e$ ,  $v$ .

$$r \cdot \sin u = z \cdot \sqrt{D_x^2 + D_y^2 + D_z^2} : \sqrt{D_x^2 + D_y^2}$$

$$r \cdot \cos u = (y \cdot D_x - x \cdot D_y) : \sqrt{D_x^2 + D_y^2}$$

Hence:  $r$ ,  $u$  and  $\omega = u - v$ ,  $\tilde{\omega} = \omega + \Omega$ .

$$\operatorname{tg} \frac{1}{2} E = \operatorname{ctg} (45^\circ + \frac{1}{2}\varphi) \cdot \operatorname{tg} \frac{1}{2} v$$

$$E - e \cdot \sin E = M = \mu(t - T)$$

Hence:  $E$ ,  $M$  and  $T$  (perihelion time of the Comet).

#### § 4. The heliocentric motion of Comet 1906 IV in the period of its sojourn in Jupiter's predominance sphere since 18 January till 27 June 1954.

As initial heliocentric equatorial orbital elements of the Comet resulting from preceding computations the following elements were accepted:

$$M \ 128^\circ 39' 52'' \cdot 15 \quad 1954. \text{ I. } 18.0 \text{ U. T.} \quad \begin{cases} \tilde{\omega} \ 282^\circ 13' 47'' \cdot 54 \\ \Omega \ 342^\circ 05' 29'' \cdot 16 \\ i \ 22^\circ 15' 57'' \cdot 27 \end{cases} \begin{cases} 1950 \cdot 0 \\ \text{Equator} \end{cases}$$

The corresponding ecliptical elements for the position of the Comet's orbit were:

$$\begin{cases} \tilde{\omega} \ 283^\circ 36' 53'' \cdot 63 \\ \Omega \ 252^\circ 11' 18'' \cdot 49 \\ i \ 7^\circ 01' 45'' \cdot 91 \end{cases} \begin{cases} 1950 \cdot 0 \\ \text{Ecliptic} \end{cases}$$

The last elements are given here for their later comparison with analogous final values (for 1954. VI. 27).

Below are given the perturbations of the orbital elements of the Comet in its heliocentric motion caused by Jupiter and Saturn in the period 1954. I. 18.0 — 1954. VI. 27.0 U. T. (to be added to the above values of the equatorial elements for the epoch 1954. I. 18).

	Jupiter	Saturn	$\Sigma$
$\Delta M$	- 4265''04	- 0''12	- 4265''16
$\Delta \mu$	+ 0'39273	+ 0 00601	+ 0'39874
$\Delta \varphi$	+ 1775'20	+ 2'96	+ 1778'16
$\Delta \tilde{\omega}$	+ 6650'26	- 0'94	+ 6649'32
$\Delta \Omega$	+ 96568'60	- 0'42	+ 96568'18
$\Delta i$	- 3299'60	+ 0'03	- 3299'57

§ 5. The jovicentric motion of Comet 1906 IV in the period of its sojourn in Jupiter's predominance sphere from 18 January till 27 June 1954.

The computations were made according to indications given in Chapters 1, 2, 3.

First of all for the equidistant epochs 1954. I. 3'0, 8'0, 13'0, 18'0, 23'0 and 28'0 the heliocentric equatorial coordinates of Jupiter  $x_1, y_1, z_1$  and their derivatives  $x'_1, y'_1, z'_1$  have been calculated by interpolation with the aid of the *American Ephemeris*. They are included in Table I which contains also the perturbed heliocentric equatorial coordinates of the Comet  $x, y, z$  resulting from the preceding heliocentric calculus as well as their derivatives  $x', y', z'$  obtained according to the formulae of Chapter 1. In the third part of the same Table I, appear the jovicentric elements of the Comet computed in accordance with section 1. c. The Comet's jovicentric elements for the epoch 1954. I. 18'0 were considered henceforth as initial, and four other sets of elements as approximate for further computations which were performed as explained in Chapter 2.

On the basis of the initial values of the Comet's jovicentric equatorial orbital elements:

$$\begin{aligned} N & 231^0 47' 13'' .68 \quad 1954. \text{ I. } 18'0 \text{ U. T.} & \tilde{\omega} & 298^0 22' 25'' .16 \\ \mu & 6492'' .61796 & \Omega & 26 13 14'22 \\ e & 5'6221 7197 & i & 105 41 07'76 \end{aligned} \left. \begin{array}{l} \\ \\ \end{array} \right\} \begin{array}{l} 1950'0 \\ \text{Equator} \end{array}$$

the following perturbations by the Sun and Saturn have been found.

The perturbations of the jovicentric equatorial orbital elements of Comet 1906 IV in the period  
1954 I. 18'0 — 1954. VI. 27 U. T.

	Jupiter	Saturn	$\Sigma$
$\Delta N$	- 17055''52	- 0''34	- 17055''86
$\Delta \mu$	- 144 20289	- 0'00126	- 144'20415
$\Delta e$	- 0'0482 1363	- 0'0000 0005	- 0'0482 1368
$\Delta \tilde{\omega}$	+ 2662'37	+ 0'08	+ 2662'45
$\Delta \Omega$	- 1253'41	0'00	- 1253'41
$\Delta i$	- 2703'27	- 0'05	- 2703'32

**Vol. 10**      *The Motion of P/Comet 1906 IV (Kopff)*      217

Table I.  
The heliocentric coordinates and their derivatives for Jupiter and Comet 1906 IV (Kopff) and its corresponding jovicentric elements used for further computation of perturbations caused by the Sun and Saturn in the jovicentric motion of the Comet.

0 <sup>h</sup> U.T.		$x_4$		$x'_4$		$y_4$		$y'_4$		$z_4$	
1954 I.	3	+0.6137	49464	-0.0075	839863	+4.6610	86880	+0.0010	979844	+1.9846	20554
8	+0.5758	12796	-0.0075	906094	+4.6664	46934	+0.0010	460360	+1.9878	47579	+0.0006
13	+0.5378	44065	-0.0075	968033	+4.6715	46231	+0.0009	940822	+1.9909	63953	+0.0006
18	+0.4998	45476	-0.0076	025688	+4.6763	86753	+0.0009	421268	+1.9939	69614	+0.0005
23	+0.4618	19110	-0.0076	079064	+4.6809	67498	+0.0008	901716	+1.9968	64505	+0.0005
28	+0.4237	67125	-0.0076	128164	+4.6852	18876	+0.0008	382206	+1.9996	48580	+0.0005

J U P I T E R											
P / C O M E T 1906 IV (K O P F F)											
		$x$		$x'$		$y$		$y'$		$z$	
1954 I.	8	+0.3314	60572	-0.0048	993523	+4.5948	57381	+0.0024	748299	+1.8319	39887
13	+0.3069	86944	-0.0048	898206	+4.6071	00957	+0.0024	229254	+1.8335	81274	+0.0003
18	+0.2825	65060	-0.0048	790884	+4.6190	86245	+0.0023	712657	+1.8351	58233	+0.0003
23	+0.2581	97385	-0.0048	671338	+4.6308	13377	+0.0023	197994	+1.8366	79222	+0.0002
28	+0.2338	94134	-0.0048	539463	+4.6422	84600	+0.0022	684659	+1.8381	51629	+0.0002

P / C O M E T 1906 IV (K O P F F)											
		$\Omega$		$i$		$N$		$\mu$		•	
		$\tilde{\Omega}$	$\Omega$	$i$	$N$	$\mu$	$\mu$	$\mu$	$\mu$	$\mu$	$\mu$
1954 I.	8	298° 29'	" 57.37	26° 21'	" 42.61	105° 52'	" 54.42	-146° 05'	" 40.6	6487"	99809
13	298	26	00.94	26	17	21.65	105	46	38.97	-137	09 21.8
18	298	22	25.16	26	13	14.22	105	41	07.76	-128	12 46.3
23	298	19	10.29	26	09	20.17	105	36	18.76	-119	16 00.0
28	298	16	16.08	26	05	39.78	105	32	08.34	-110	18 52.8

Thus, taking into consideration the equation:

$$N_{1954. \text{ VI. } 27} = N_{1954. \text{ I. } 18} + \mu_{1954. \text{ I. } 18} \cdot 160 + \Delta N$$

the following final system of the jovicentric equatorial orbital elements of the Comet resulted:

$$\left. \begin{array}{l} N 155^{\circ} 36' 36'' .70 \quad 1954. \text{ VI. } 27^{\circ} \text{ U. T.} \\ \mu \quad 6348.41381 \\ e \quad 5.57395830 \end{array} \right\} \begin{array}{l} \tilde{\omega} 299^{\circ} 06' 47'' .61 \\ \Omega \quad 25^{\circ} 52' 20'' .81 \\ i \quad 104^{\circ} 56' 04'' .44 \end{array} \begin{array}{l} 1950.0 \\ \text{Equator} \end{array}$$

### §. 6. The regularity of the course of the jovicentric calculus.

Table 2.

The distances of Comet 1906 IV from the Sun and Jupiter according to the jovicentric (*j*) and heliocentric (*h*) method.

The unit of columns (*j*) — (*h*) is  $10^{-7}$ .

Date	from the Sun ( <i>j</i> )	( <i>j</i> ) - ( <i>h</i> )	from Jupiter ( <i>j</i> )	( <i>j</i> ) - ( <i>h</i> )
1954. I. 8	4.9576788	- 5	0.2985628	+ 33
13	4.9680620	- 1	0.2867354	+ 3
18	4.9783136	0	0.2751639	+ 5
23	4.9884360	+ 4	0.2638861	- 20
28	4.9984313	+ 3	0.2529457	+ 4
II. 2	5.0083018	+ 2	0.2423933	- 4
7	5.0180496	+ 3	0.2322873	- 5
12	5.0276766	- 6	0.2226942	- 7
17	5.0371842	+ 6	0.2136893	+ 3
22	5.0465740	- 6	0.2053569	- 18
27	5.0558463	+ 15	0.1977886	- 53
III. 4	5.0650008	- 22	0.1910822	- 40
9	5.0740357	+ 11	0.1853382	- 16
14	5.0829481	- 16	0.1806544	+ 14
19	5.0917334	- 10	0.1771205	- 11
24	5.1003857	+ 5	0.1748104	+ 2
29	5.1088974	+ 2	0.1737756	+ 1
IV. 3	5.1172604	+ 1	0.1740398	- 4
8	5.1254658	+ 1	0.1755962	- 3
13	5.1335050	- 4	0.1784084	- 2
18	5.1413706	+ 3	0.1824140	+ 1
23	5.1490556	- 13	0.1875312	+ 0
28	5.1565551	+ 4	0.1936655	+ 5
V. 3	5.1638651	+ 3	0.2007166	+ 12
8	5.1709834	+ 4	0.2085844	+ 15
13	5.1779086	+ 7	0.2171727	+ 14
18	5.1846406	+ 11	0.2263924	+ 15
23	5.1911797	+ 11	0.2361626	+ 21
28	5.1975272	+ 11	0.2464111	+ 35
VI. 2	5.2036844	+ 18	0.2570743	+ 28
7	5.2096532	+ 14	0.2680968	+ 36
12	5.2154351	+ 19	0.2794303	+ 28
17	5.2210323	+ 27	0.2910331	+ 44
22	5.2264466	+ 31	0.3028692	+ 32
27	5.2316793	+ 39	0.3149074	+ 35

Before we return to the heliocentric system of the Comet's elements it is appropriate to make some remarks.

The superiority of the jovicentric method by applying it for the time of the sojourn of the Comet in Jupiter's predominance sphere can be confirmed in many ways. One of them is to confront the values of the distances of the Comet from Jupiter and the Sun obtained in both methods (Table 2).

It is easily seen by forming the differences that the run of the numbers concerning the jovicentric motion of the Comet is very regular, what cannot be said about the course of the corresponding numbers in the heliocentric method. This is caused undoubtedly by the uncertainty of K, a quantity obtained as difference of great numbers of the same order. The differences  $(j) - (h)$  at the end of the Table seem to reveal their systematic character.

#### § 7. Return to the heliocentric system. Comparison of the practical results of both methods.

Referring to the results of Chapter 5 and following the indications of Chapter 3 we find by interpolation for the final epoch 1954. VI. 27<sup>o</sup> U. T.:

$$\begin{aligned}x_1 &= -0.719244657 \\y_1 &= +4.694794290 \\z_1 &= +2.031672716\end{aligned}$$

$$\begin{aligned}x'_1 &= -0.007565163892 \\y'_1 &= -0.000703878348 \\z'_1 &= -0.000117003162\end{aligned}$$

then

$$\begin{aligned}\xi &= +0.241171608 \\ \eta &= +0.155435128 \\ \zeta &= -0.129780076\end{aligned}$$

$$\begin{aligned}\xi' &= +0.002737562186 \\ \eta' &= +0.001154679484 \\ \zeta' &= +0.000583537845\end{aligned}$$

and returning thus to the heliocentric equatorial system we obtain:

$$\left. \begin{array}{l} M 153^{\circ} 38' 51'' 68 \quad 1954. \text{VI. } 27^{\circ} \text{ U. T.} \quad \tilde{\omega} 284^{\circ} 04' 36'' 96 \\ \mu \quad 589'' 17418 \quad \Omega \quad 8^{\circ} 54' 57'' 40 \\ \varphi \quad 37^{\circ} 15' 40'' 40 \quad i \quad 21^{\circ} 20' 57'' 63 \end{array} \right\} 1950^{\circ} \text{ Equator}$$

and in reference to the ecliptic:

$$\left. \begin{array}{l} \tilde{\omega} 283^{\circ} 24' 29'' 24 \\ \Omega \quad 125^{\circ} 44' 56'' 96 \\ i \quad 3^{\circ} 59' 11'' 55 \end{array} \right\} 1950^{\circ} \text{ Ecliptic}$$

	Jovic. eq. System	Helioc. eq. System	$(j) - (h)$
$\Delta M$	- $1^{\circ} 11' 04'' 56$	- $1^{\circ} 11' 05'' 16$	+ $0'' 60$
$\Delta \mu$	+ $0'' 39858$	+ $0'' 39874$	- $0.00016$
$\Delta \varphi$	+ $0^{\circ} 29' 37'' 98$	+ $0^{\circ} 29' 38'' 16$	- $0.18$
$\Delta \tilde{\omega}$	+ $1^{\circ} 50' 49' 41$	+ $1^{\circ} 50' 49' 32$	+ $0.09$
$\Delta \Omega$	+ $26^{\circ} 49' 28' 24$	+ $26^{\circ} 49' 28' 17$	+ $0.07$
$\Delta i$	- $0^{\circ} 54' 59' 64$	- $0^{\circ} 54' 59' 57$	- $0.07$

A comparison of the results obtained in Chapters 4 and 7 gives us the perturbations of the jovicentric orbital elements of the Comet produced by the Sun and Saturn as well as the perturbations of the heliocentric ones produced by Jupiter and Saturn in the period from 1954. I. 18 till 1954. VI. 27. They are given in the Table above.

In the light of the differences  $(j) - (h)$  it can be stated that both methods have practically led to the same results.

We supply the last results with the following corrections to the Comet's elements  $\tilde{\omega}$ ,  $\Omega$ ,  $i$  referred to the ecliptic, taking into consideration the presence of three bodies: the Sun, Jupiter and Saturn:

$$\left. \begin{array}{l} \Delta\tilde{\omega} = 0^0 12' 24'' .39 \\ \Delta\Omega = 126^{\circ} 26' 21'' .53 \\ \Delta i = 3^{\circ} 02' 34'' .36 \end{array} \right\} \text{Ecliptic}$$

### § 8. Conclusions.

In consequence of the preceding investigations it can be said that both methods, when carefully applied, yield the same results. But in the case of a close approach of a comet to Jupiter the jovicentric method wins a decisive superiority over the heliocentric one; moreover it may even advantageously be applied somewhat beyond Jupiter's predominance sphere.

It would not be superfluous to insist on the subject.

As a comet does approach and then penetrates this sphere, the disturbing influence of the Sun considered in the jovicentric system shows a regular run. On the contrary, the perturbations of the heliocentric motion of the comet produced by Jupiter grow then rapidly and their computation causes many difficulties because of the necessity of changing frequently the integrating intervals which is often realized in inadequate epochs.

On the contrary, in computing the motion of a comet, which travels in Jupiter's predominance sphere, the problem of length of the integrating interval does rather not exist when the motion of the comet is considered in the jovicentric system.

However, it is of great importance to establish always a most accurate passage from the heliocentric system to the jovicentric one and *vice versa*.

### REFERENCES:

- [1] F. Kępiński: The Motion of the P/Comet 1906 IV (Kopff), *Acta Astr.* Vol. 8, 193, 1958.
- [2] M. Kamiński: The Motion of Comet P/Wolf 1 in the Proximity of Jupiter's Activity Sphere, *A. A.*, Vol. 7, 159, 1957.

Astronomical Institute  
of the Polish Academy of Sciences,  
Comet Section.  
Warsaw, May 1960

F. Kępiński

## Comet P/Wolf I in 1958

by

M. Kamiński

§ 1. On its tenth return to the Sun, this Comet was placed very unfavourably for observations, since on its perihelion passage

$T_{10} = 1959 \text{ March } 21^{\text{st}} 916 \text{ U. T.}$

it was situated beyond the Sun (v. graph). Nevertheless the Big Eye at Mount Palomar was successful in picking it up on photographic plates on 13th June 1958, when it was near its opposition. Two weeks later, indefatigable Elizabeth Roemer photographed it at Flagstaff, Arizona, with the help of the 40-inch reflector, and watched it up to the beginning of November 1958, when the Comet became so faint that it could not be detected on photographic plates.

Now, on the day of its discovery on 13th June 1958, its apparent brightness measured with the 200 inch telescope of Mount Palomar, was

photovisual	$20^m 4$
photographic	$20^m 9$

The distances  $r$  of the Comet from the Sun and  $\Delta$  — from the Earth were considerable:

$$r = 3^{\circ}098 \quad \Delta = 2^{\circ}429$$

From the known formula

$$H_{\text{app.}} = H_{\text{abs.}} + 5 \log \Delta + 2.5 k \lg r \quad k = 4$$

we find

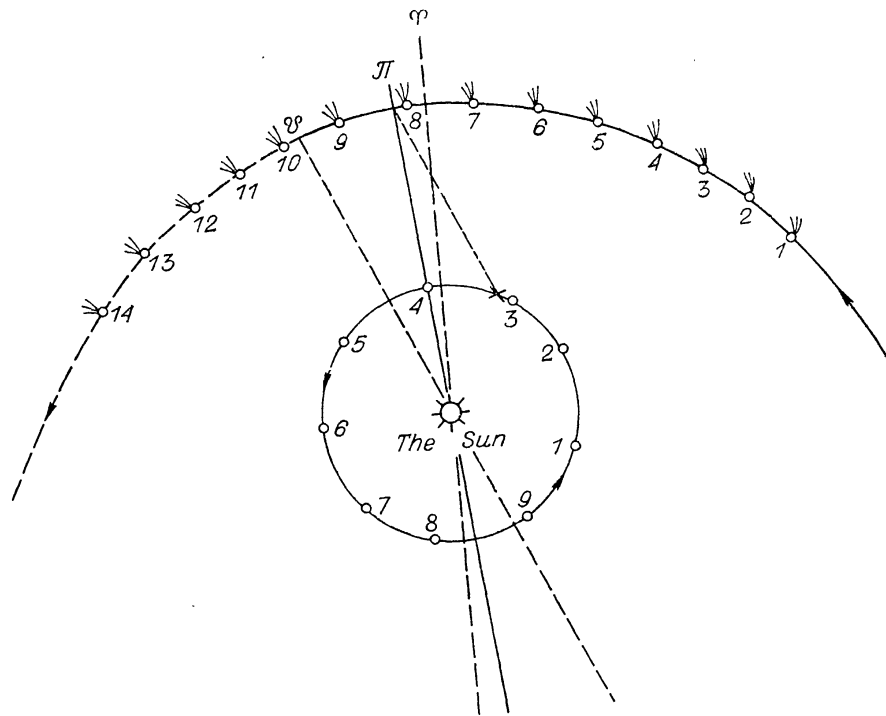
$$H_{\text{app.}} = H_{\text{abs.}} + 6^m 84$$

Hence

$$\begin{aligned} H_{\text{phot.}} &= 14^m 1 \\ H_{\text{phot v.}} &= 13^{\circ}6 \end{aligned}$$

On comparing these values for  $H_{\text{abs.}} = H_0$  with the preceding ones for the period 1925—1942—1958, we note that its absolute photographic brightness  $H_0^{\text{pg}}$  during the last 16 years seems to remain without alteration:

1925	$H_0 = 10^m 3$
1933/34	$H_0 = 12^{\circ}1$
1942	$H_0 = 14^{\circ}1$
1950/51	$H_0 = 13^{\circ}3$
1958	$H_0^{\text{pg}} = 14^{\circ}1$
	$H_0^{\text{v.}} = 13^{\circ}6$



Corresponding positions of the Earth and Comet P/Wolf I during its apparition in 1958.

Figures 1, 2, 3 on the circumference of the Earth's orbit and on the Comet's orbit indicate the mutual positions of these celestial bodies in their orbits, for the moments:

1	1958 June 6	6	1958 Dec. 23
2	July 16	7	1959 Feb. 1
3	Aug. 25	8	Mar. 13
4	Oct. 4	9	Apr. 22
5	Nov. 13		

10	the Comet on 1959 June 1
11	" " " July 11
12	" " " Aug. 20
13	" " " Sept. 29
14	" " " Nov. 8

The cross + near 3 on the Earth's orbit indicates the position of the Earth at the moment

$$T_{11} = 1967 \text{ Aug. 27}$$

of the next perihelion passage of the Comet.

Consequently, one can assume that for the next perihelion passage of the Comet

$$T_{11} = 1967 \text{ Aug. 27} = 1967.65$$

its absolute brightness  $H_0$  will be nearly  $14^{m.1}$  (v. below § 5).

§ 2. The system of elements  $Q_5^{\text{rev}}$  for 1950 Oct. 6<sup>o</sup> U. T. was taken as basis for the comparison of the theory of the Comet with its observations in 1958:

Epoch and Osculation  
1950 Oct. 6<sup>o</sup> U. T.

$Q_5^{\text{rev.}}$	$M 357^{\circ} 55' 58'' \cdot 17$	$\Omega 203^{\circ} 52' 45'' \cdot 50$
	$\varphi 23 21 5 \cdot 72$	$\pi 5 1 29 \cdot 71$
	$n 421'' \cdot 5801$	$i 27 18 58 \cdot 41$

$1950^{\circ} 0$

This system represents the observations of the Comet in 1950—1951 very well [1]. On completing it with the sums  $\Sigma_6 \delta \Theta$  of perturbations due to Venus, the Earth, Mars, Jupiter, Saturn and Uranus [2] from the epoch of the above system up to the actual dates of its Ephemeris for June and July 1958, we obtained the perturbed Ephemeris as follows:

### The Ephemeris for $0^{\text{h}}$ U. T.

1958	$\alpha_{1950.0}$	$\delta_{1950.0}$	r	$\Delta$	Light - Time
June	10.0	20 <sup>h</sup> 12 <sup>m</sup> 36. <sup>s</sup> 67	+16°20'19.3	3.1093	2.4680
	11.0	20 12 28.09	+16 29 1.9	3.1058	2.4563
	12.0	20 12 18.34	+16 37 36.2	3.1024	2.4448
	13.0	20 12 2.46	+16 46 2.0	3.0989	2.4334
	14.0	20 11 55.41	+16 54 19.1	3.0955	2.4221
	15.0	20 11 42.22	+17 2 26.8	3.0920	2.4110
	16.0	20 11 27.88	+17 10 24.9	3.0886	2.4000
	17.0	20 11 12.42	+17 18 13.2	3.0853	2.3891
	18.0	20 10 55.84	+17 25 51.5	3.0819	2.3784
	19.0	20 10 38.14	+17 33 19.3	3.0785	2.3679
	20.0	20 10 19.35	+17 40 36.5	3.0751	2.3575
	21.0	20 9 59.50	+17 47 42.5	3.0716	2.3473
	22.0	20 9 38.58	+17 54 37.1	3.0682	2.3372
	23.0	20 9 16.60	+18 1 19.8	3.0648	2.3273
	24.0	20 8 53.68	+18 7 50.6	3.0614	2.3176
	25.0	20 8 29.71	+18 14 9.0	3.0581	2.3080
	26.0	20 8 4.61	+18 20 14.9	3.0547	2.2986
July	8.0	20 1 55.34	+19 15 16.6	3.0145	2.1992
	9.0	20 1 19.50	+19 18 12.5	3.0112	2.1922
	10.0	20 0 43.02	+19 20 51.8	3.0079	2.1853
	11.0	20 0 5.94	+19 23 14.5	3.0046	2.1786
	12.0	19 59 28.33	+19 25 20.6	3.0013	2.1721
	13.0	19 58 50.20	+19 27 9.8	2.9980	2.1658
	14.0	19 58 11.59	+19 28 41.8	2.9947	2.1596
	15.0	19 57 32.56	+19 29 56.4	2.9914	2.1537
	16.0	19 56 53.09	+19 30 53.5	2.9881	2.1479

§ 3. The Comet's positions during its apparition in 1958 were very unfavourable for observation as can be seen from the graph above. During its opposition to the Sun, in the middle of summer 1958, its distances from the Sun and from the Earth were comparatively great, as stated above. Nevertheless, it was found on Mount Palomar plates and — some days later — at the Flagstaff Station of the U. S. Navy. Measurements of the plates yielded the following exact positions:

	1958. U. T.	$\alpha_{\text{obs.}}^{1950.0}$	$\delta_{\text{obs.}}^{1950.0}$	Note
1	June 13'40903	20 <sup>h</sup> 12 <sup>m</sup> 1 <sup>s</sup> .52	+16°49'24.1''	Mount Palomar 200-inch reflector
2	13'42708	20 12 1.28	+16 49 32.8	
3	24'32569	20 8 44.81	+18 9 52.3	
4	24'40672	20 8 42.75	+18 10 23.8	Flagstaff Station of the U. S. Naval Observatory with 40-inch reflector
5	July 10'21027	20 00 34.13	+19 21 20.0	
6	10'28299	20 00 31.43	+19 21 31.1	

Positions 1, 2 were published in *Circular* 1651 of the I. A. U. 8th July 1958. Positions 3, 4, 5, 6 were taken from a letter of E. Roemer to the author, dated May 18th 1959 [3]. This letter contains also the following approximate positions of the Comet, with some additional remarks:

Sept. 15·20925 — barely possible image; exceedingly rich field.

	1958 U. T.	$\alpha$ obs. 1950·0	$\delta$ obs. 1950·0	
7	Oct. 8·12578	19 <sup>h</sup> 43 <sup>m</sup> .10	+ 8° 14'·4	
8	8·19208	19 43 .15	+ 8 13 .7	
9	14·12303	19 47 .87	+ 7 14 .5	Uncertainty $\pm 0^m 05, 0' 5$
10	14·18951	19 47 .93	+ 7 13 .8*)	

\*) Image of Comet superposed a fairly faint star trail.

Nov. 9 — Comet not found; pair of plates. Endeavours to photographing it in August and in October 1959 were unsuccessful [4].

§ 4. After correcting the observed positions for the influence of aberratio fixarum and parallaxes, the author found:

	1958 U. T.	Aberr. fix. in $\alpha$ in $\delta$	Parall. in $\alpha$ in $\delta$	$\alpha$ obs. def.	$\delta$ obs. def.
1	June 13·40903	+ 8 ·08	- 5''	— 0'03	+ 16 49 20''
2	13·42708	+ 8 ·08	- 5''	— 0'02	+ 16 49 28·8
3	24·32569	+ 8 ·25	- 2'9	— 0'09	+ 18 9 50·6
4	24·40672	+ 8 ·25	- 2'9	+ 0'02	+ 18 10 21·2
5	July 10·21027	+ 8 ·40	+ 0'7	- 0'18	+ 19 21 22·2
6	10·28299	+ 8 ·40	+ 0'7	- 0'09	+ 19 21 31·0

On the other hand, taking into account the light time, we find from the perturbed Ephemeris given in § 2 the following computed positions of the Comet and their differences from the observed ones:

	1958 U. T.	$\alpha$ cal. 1950·0	$\delta$ cal. 1950·0	$(\alpha^o - \alpha^c) \cos \delta$	$\delta_c - \delta_o$
1	June 13·39501	20 12 2·79	+ 16 49 19·0	- 0'21	+ 8'
2	13·41306	20 12 2·58	+ 16 49 28·0	- .23	+ 0·8
3	24·31233	20 8 46·30	+ 18 9 50·2	- .32	+ 0·4
4	24·39336	20 8 44·37	+ 18 10 20·9	- .34	+ 0·3
5	July 10·19767	20 0 35·74	+ 19 21 21·3	- .38	+ 0·9
6	10·27039	20 0 33·05	+ 19 21 32·0	- .30	- 1·0

We see that the differences are exceedingly small; they are of the same order as in the previous apparition of the Comet in 1950 — 1951.

One can form 3 normal places of the Comet, corresponding to 3 normal differences namely:

	1958 U. T.	$(\alpha^0 - \alpha^\circ) \cos \delta$	$\delta^0 - \delta^\circ$	$\alpha$ nor. 1950.0	$\delta$ nor. 1950.0
1	June 13.0	- 0.22 <sup>s</sup>	+ 1.0 <sup>"</sup>	20 12 2.23 <sup>h m s</sup>	+ 16 46 3 <sup>0 0"</sup>
2	24.0	- 0.33	+ 0.4	20 8 53.34	+ 18 7 51.0
3	July 10.0	- 0.34	0.0	20 0 42.67	+ 19 20 51.8

The approximate positions of the Comet for 1958, Oct. 8 and Oct. 14, cannot be used for correcting the theory of the motion of this Comet. They are:

	1958 U. T.	Aberr. fix. in $\alpha$ in $\delta$	$\alpha$ obs. def.	$\delta$ obs. def.	$\alpha^0 - \alpha^\circ$	$\delta^0 - \delta^\circ$
7	Oct. 8.12579	+ 0.2 <sup>s</sup> + 10 <sup>"</sup>	19 43 6 <sup>h m s</sup>	+ 8 14.6 <sup>"</sup>	- 0.03 <sup>m</sup>	- 0.2 <sup>'</sup>
8	8.19208	+ 0.2 <sup>s</sup> + 10 <sup>"</sup>	19 43 9	+ 8 13.9	- 0.03 <sup>m</sup>	- 0.2 <sup>'</sup>
9	14.12303	+ 0.1 <sup>s</sup> + 10 <sup>"</sup>	19 47 52	+ 8 14.7 <sup>"</sup>	- 0.02 <sup>m</sup>	+ 0.3 <sup>'</sup>
10	14.18951	+ 0.1 <sup>s</sup> + 10 <sup>"</sup>	19 47 56	+ 8 14.0 <sup>"</sup>	- 0.02 <sup>m</sup>	+ 0.3 <sup>'</sup>

These deviations seem to be perhaps too great, but in the light of the note of E. Roemer, they remain within the limits of the exactness of measurements (uncertainty  $\pm 0^m.05$ ;  $0'5$ ).

§ 5. On comparing the normal places with those obtained by computation in the period 1925—1958, we got the following Table I.

Table I

Comparison of the theory based on systems of elements  
 $Q$ , with normal places for the period 1925—1958

No.	U. T.	$\Delta \alpha \cos \delta$	$\Delta \delta$	Num.	No.	U. T.	$\Delta \alpha \cos \delta$	$\Delta \delta$	Num.	
1	1925	July 18.0	- 0.01 <sup>s</sup>	- 0.4 <sup>"</sup>	4	1942	Nov. 7.0	+ 0.11 <sup>s</sup>	+ 1.8 <sup>"</sup>	3
2		Aug. 19.0	- 0.12	0.0	8		Dec. 12.0	- 0.14	- 0.4	2
3		Sept. 14.0	+ 0.05	- 0.5	3					
4		Oct. 12.0	- 0.04	- 1.6	4					
5		Nov. 12.0	0.00	+ 1.1	3					
6		Dec. 19.0	+ 0.16	+ 0.7	4					
7	1933	July 27.0	- 0.04	- 0.4	5	1950	June 19.0	- 0.16	+ 0.8	4
8		Aug. 23.0	0.00	+ 0.4	3		July 21.0	- 0.25	- 0.4	4
9		Sept. 16.0	+ 0.07	+ 0.6	2		Aug. 16.0	- 0.28	+ 1.1	4
10		Nov. 11.0	+ 0.02	- 0.3	2		Sept. 11.0	- 0.25	+ 0.7	3
11		Sept. 11.0	+ 0.11	- 0.3	6		Oct. 10.0	- 0.17	+ 0.7	1
12		Oct. 15.0	0.00	+ 0.4	1		Nov. 5.0	- 0.15	+ 0.1	3
13	1934	Dec. 11.0	- 0.08	- 1.7	2		Dec. 13.0	- 0.29	+ 1.2	2
							Jan. 7.0	- 0.14	+ 0.3	3
24	1958	June 13.0	- 0.22	+ 1.0	2	1958	June 24.0	- 0.33	+ 0.4	2
25		July 10.0	- 0.34	0.0	2		July 10.0	- 0.34	0.0	2
26										

One can see from the Table above that the theory of the motion of Comet P/Wolf I during the period 1925—1958 appears to be very satisfactory.

It is moreover to be noted that the deviations 1—15 were obtained by an elaborate linkage and adjustment of the reappearances of the Comet during 1925—1942. On the other hand, deviations

16—26 correspond to the system  $Q_5^{\text{rev}}$  which was not yet linked and adjusted with the preceding systems  $Q_1, Q_2, Q_3, Q_4$ . Nevertheless one can be sure that the adjustment of all the residuals in the period 1925—1958 would change very little the systems  $Q_1, Q_2, Q_3, Q_4, Q_5^{\text{rev}}$ . It is not excluded that this adjustment can cause the apparition of a very small deceleration term in the Comet's motion.

Finally it is to be noted also [6] that the variation of the mean anomaly  $M$  in the system of elements  $Q_5^{\text{rev}}$  for 1950 Oct. 6 of one second of arc only will reduce the deviations in 1950—1951 almost to zero, as well as diminish considerably the small residuals in 1958. Now the perturbation  $\delta M$  in the mean anomaly of the Comet due to Jupiter in the period 1942 June 10—1950 Oct. 6 was comparatively great, amounting to

$$\delta M = -7660'' \cdot 26$$

Thus, one second of arc is nearly 1/8000 of the value above, being almost at the limit of exact computations performed by the Method of Variation of Arbitrary Constants, and probably also by other methods.

In any case, the deviations in Table I indicate that the systems of elements  $Q_i$  are very exact and can be taken as the basis for the precise computations of perturbations in the motion of this Comet during 1960—1967, caused by six planets of our solar system.

The position of the Comet for its next apparition in 1967 will be favourable enough for observation (v. graph). The observations — provided the Comet will be found — shall indicate, whether and in what degree — an adjustment will be necessary.

#### REFERENCES:

- [1] M. Kamiński. Comet P/Wolf I in 1950—1951. *A. A.* 6, p. 74, 1956.
- [2] M. Kamiński, Researches on the Motion of Comet P/Wolf I. Part XVII. *A. A.* 8, p. 8—55, 1957.
- [3] Letter of Miss Dr Elizabeth Roemer to the author dated May 18, 1959.
- [4] Letter of Miss Dr E. Roemer to the author dated Febr. 8, 1960.
- [5] M. Kamiński — l. c. [1], p. 79.

Astronomical Institute of the  
Polish Academy of Sciences  
Comet Section  
Cracow, 9th March 1960.

M. Kamiński

## Photographic Measurements of Polarization in the Region of the Association III Cephei

by

K. Serkowski

### SUMMARY

The method of determining stellar polarization photographically by means of two crossed calcite plates is described. Two images of each star are formed which have the same shape and are situated at the same distance from the surface of the calcite. Polarization of 70 stars in the region of the association III Cephei was determined by this method. The mean error of the amount of polarization determined from 16 exposures is  $\pm 0.^m013$ .

#### 1. Crossed calcite plates.

Among different methods of determining stellar polarization photographically the best results were obtained by photographing the sky through a plane-parallel calcite plate. This method was used by Markowitz and Hall (1950), Markowitz (1951), Gossner (1952), Behr (1955) and van den Bergh (1956), and criticized by Loden (1958) and Bartl (1959). The light of a star after passing through the calcite plate forms two images of the star on the photographic plate. The shape of these two images is not identical; the extraordinary image is deformed by astigmatism. The plane in which the "circles of the least confusion" for the extraordinary beams are formed is not identical with the focal plane for the ordinary beams. For this reason even very small changes in focusing cause large changes in the difference of the photographic density of the two images, especially when the focal ratio of the telescope is small.

To avoid these errors Serkowski (1958a) and, independently, Bartl (1959) proposed to use two identical plane-parallel calcite plates oriented so that their principal sections are perpendicular to one another. The beam of light which is ordinary in the first calcite plate is extraordinary in the second one and vice versa. Hence both images of a star are formed by these two plates in the same plane perpendicular to the direction of the initial light ray and both images have the same shape. The images are circular if the focusing is correct.

#### 2. Absolute determination of position angles.

The principal sections of the two calcite plates do not need to be exactly perpendicular. If the principal sections are not exactly

perpendicular, we obtain for bright stars not only two bright images, but also two faint ones which should be extinguished when the principal sections are exactly perpendicular. These faint images may be useful for absolute determination of the position angles of the plane of vibration of stellar light.

Let us rotate both calcite plates together until one obtains the minimum brightness of the image formed by the beam of light which is ordinary in both calcite plates. The position angle of the plane of vibration is now equal to the position angle of the line joining the two images formed by the beams which are ordinary in the second calcite plate. It is more convenient to measure the position angle of the line joining the two brighter images on the photographic plate; it is larger by some angle  $\alpha$  than the position angle defined in the previous sentence. The tangent of this angle  $\alpha$  is equal to the ratio of the distance between the two fainter images of a star and the distance between the two brighter images.

### 3. Observations.

The first trials for measurement of polarization photographically with two crossed calcite plates of small diameter kindly supplied by Professor A. Gaweł were made by the author during the summer of 1956. The following year two identical calcite plates 60 mm in diameter by 4 mm thick were polished for the Astronomical Observatory of Warsaw University by Dr. Steeg and Reuter Company of Bad Homburg, Germany. The distance between the two images of a star given by these crossed plates is 0.63 mm.

The central part of the association III Cephei was photographed in September 1957 with calcite plates placed near the focus of the 35 cm Hainberg astrograph at the Göttingen Observatory. The exposure time was 2 minutes on Kodak 103a-O plates. The plates were measured with an iris-diaphragm Sartorius microphotometer of the Hamburg-Bergedorf Observatory. All of the stars brighter than 11.5 ptg. within a circular area 1.0 in diameter were measured.

The area situated to the north-east of the center of the association was photographed in September 1958 with the same calcite plates attached to the 14 cm astrograph (focal ratio f/5) of the Ostrowik Station of the Astronomical Observatory of Warsaw University. Exposure time was 90 seconds on blue sensitive Agfa Astro plates. These plates were measured at the Warsaw Observatory with a type MF2 microphotometer (produced in USSR). It operates with a circular diaphragm of a constant diameter of 0.13 mm.

Both in Göttingen and in Ostrowik 8 exposures were made on each plate. These exposures were made in 8 position angles of the calcite plates each differing by 45°. In future work the author does not recommend making more than one exposure on each plate. If only one exposure is made on each plate, the mean value of the results obtained for a given star from two plates exposed at position angles of the analyser differing by 180° is very nearly free of the interfering influence of neighbouring stars.

#### 4. Accuracy of the results.

Among the stars measured 20 are contained in Hall's (1958) catalogue of photoelectric polarization measurements. The polarization of these stars is described by means of parameters (cf. Behr 1956)

$$p_x = p \cos 2\theta_E, \quad p_y = p \sin 2\theta_E,$$

which we shall call the Stokes parameters expressed in magnitudes; here  $p$  is the amount of polarization in magnitudes and  $\theta_E$  is the position angle of the plane of vibration referred to the system of equatorial co-ordinates. When comparing a series of polarization measurements it is convenient to use the parameters  $p_x$  and  $p_y$ , as their mean errors should be independent of the values of the parameters themselves.

The comparison between the values of  $p_x$  and  $p_y$  for the 20 stars mentioned, as derived from the present observations and from the mean values given by Hall (1958) is shown in Figure 1. The open

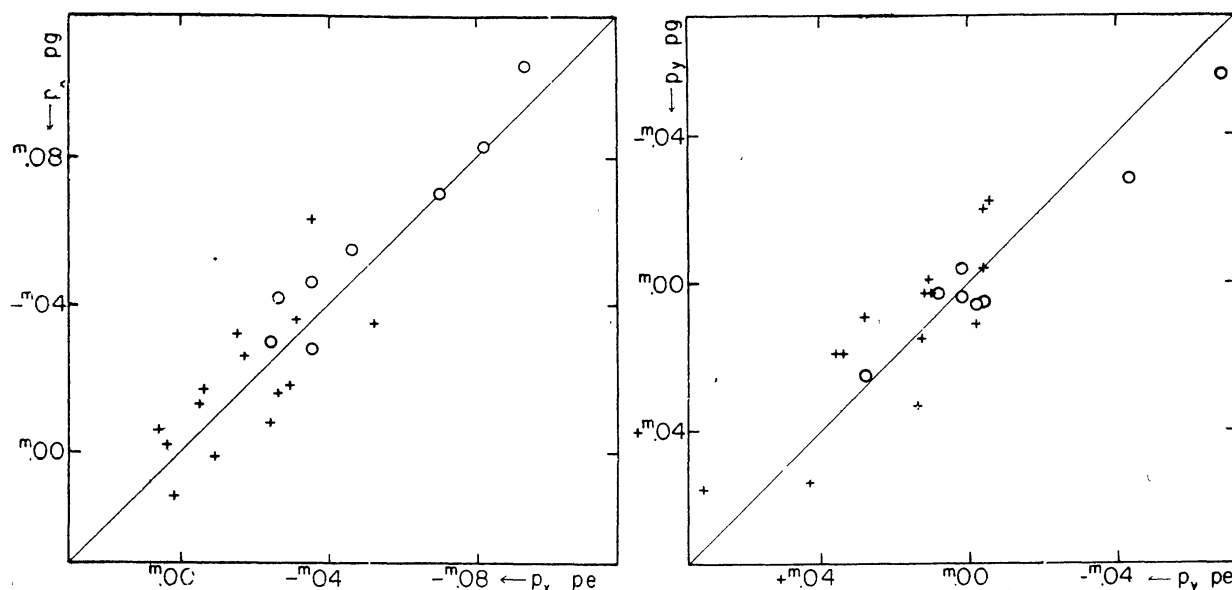


Fig. 1. The values of the Stokes parameters  $p_x$  and  $p_y$  as determined from photographic plates obtained in Göttingen (open circles) and Ostrowik (crosses) compared with those derived from photoelectric measurements given in Hall's (1958) catalogue.

circles represent the values derived from the plates obtained in Göttingen, the crosses those obtained in Ostrowik. Two stars were measured both on Göttingen and Ostrowik plates. For stars HD 216629 and 216658, separated by only 2 minutes of arc, Hall's measurements only were taken into account. Both Hall's photoelectric observations and the present photographic observations seem to show that Hiltner intermingled the results of his polarization measurements for these two stars.

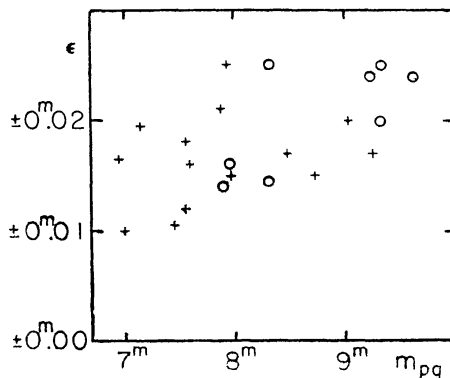


Fig. 2

Fig. 2. The root-mean-square deviations of the values of Stokes parameters given by individual plates (4 exposures for each Stokes parameter on each plate) from photoelectric data, plotted against Brodskaja (1955) photographic magnitudes. Open circles — Göttingen plates, crosses — Ostrowik plates.

It should be noted that if the exposures are made with position angles of the analyser differing by  $45^\circ$  the parameter  $p_x$  is obtained from exposures at position angles  $0^\circ$ ,  $90^\circ$ ,  $180^\circ$  and  $270^\circ$  while the parameter  $p_y$  is obtained from exposures at position angles  $45^\circ$ ,  $135^\circ$ ,  $225^\circ$ , and  $315^\circ$ . The magnitude difference between the two images of a star obtained for any exposure is equal to the corresponding Stokes parameter expressed in magnitudes.

The r. m. s. deviations of the values of Stokes parameters given by individual plates from those obtained from Hall's data are shown in Fig. 2. The r. m. s. deviation is computed for each star separately and is shown as a function of the photographic magnitude of a star taken from Brodskaja (1955) catalogue. The deviation increases with the magnitude of a star. For this reason no star fainter than 2 magnitudes from the plate limit was measured on either the Göttingen or Ostrowik plates. Since there are 4 exposures corresponding to each of the Stokes parameters on each plate, the values in Fig. 2 are the r. m. s. deviations of the values of the Stokes parameters, each of them derived from 4 exposures. Assuming that the mean error of the Stokes parameter obtained from Hall's data is  $\pm 0.^{\circ}004$  and averaging the data found in Fig. 2 we find that the mean error of the Stokes parameter determined from 4 exposures is

$$\begin{aligned} &\pm 0.^{\circ}020 \text{ for Göttingen plates,} \\ &\pm 0.^{\circ}018 \text{ for Ostrowik plates.} \end{aligned}$$

As shown by Serkowski (1958b), if the amount of polarization is several times larger than the mean error of the Stokes parameter, the mean error of amount of polarization is equal to the mean error of the Stokes parameter. Let us assume that the mean error of the Stokes parameter is inversely proportional to the square root of the number of exposures. Then we see that the mean error of the amount of polarization determined for strongly polarized stars from 32 exposures (16 for determining  $p_x$  and 16 for  $p_y$ ) is

$\pm 0.^m010$  for Göttingen plates,  
 $\pm 0.^m009$  for Ostrowik plates.

These values are about the same as those obtained for a series of 32 exposures by van den Bergh (1956).

The weighted mean difference between the position angles determined photographically and those given by Hall for 20 stars in common are

$$\theta_{pg} - \theta_{pe} = \begin{cases} -2.^o0 \pm 1.^o3 & (\text{m. e.}) \text{ for Göttingen plates,} \\ -2.^o1 \pm 3.^o7 & (\text{m. e.}) \text{ for Ostrowik plates.} \end{cases}$$

The products of the number of exposures and the square of the photographic amount of polarization were taken as weights when computing the above mean values.

### 5. Results and discussion.

All the polarization measurements in the area limited by galactic longitudes  $76^{\circ}$  and  $82^{\circ}$  and latitudes  $+2^{\circ}$  and  $+5^{\circ}$  are given in Table 1 and in Figs. 3 and 4. The first two columns of Table 1 give

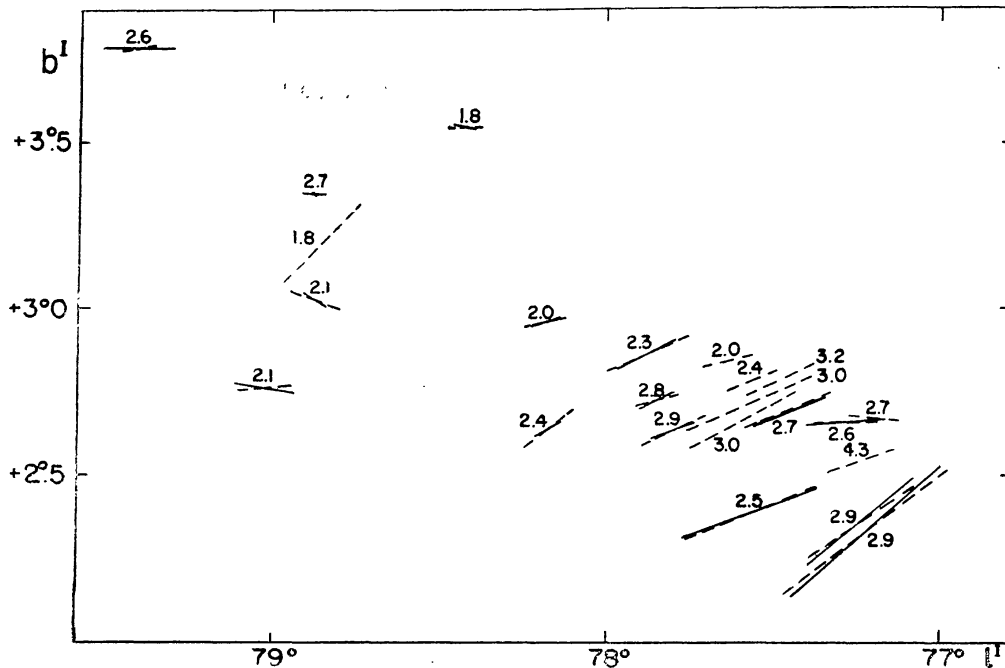


Fig. 3. Polarization of the members of association III Cephei. The length and position angle of each line indicate the relative amount of polarization and the plane of vibration, respectively. The solid lines are photoelectric measurements, the dashed lines — photographic measurements. The numbers indicate the visual absorption,  $A\gamma$ , in magnitudes, according to Table 2 of Blaauw *et. al.* (1959) paper.

the number of a star according to HD or BD and Brodskaja's (1955) catalogues. The 3rd and 4th columns give the galactic co-ordinates, the 5th the photographic magnitude according to Brodskaja and the

Table I.  
Polarization of stars in the region of the association  
III Cephei.

HD BD	Brodskaia No.	$\ell^I$	$b^I$	$m_{pg}$	n	p	$\theta_E$	$\theta_G$	$A_v$
216014	AH Cep	77° 9'	+5.3	(7.0)	16 W	0.025	66°	91°	1.8
216173	.....	77.5	4.0	(8.5)	16 W	.037	50	75	.....
+61°2352	.....	76.9	2.7	(11.4)	-	.064	109	134	4.8
.....	109	77.2	2.7	11.39	32 G	.031	61	86	2.7 m
.....	143	77.2	2.4	11.40	32 G	.066	171	15	(0.4)
216532	147	77.3	2.7	8.31	56 G	.038	69	93	2.6 m
+61°2358	149	77.4	2.9	11.29	40 G	.019	91	115	(2.1)
+61°2357	154	77.2	2.5	10.82	40 G	.044	85	109	4.3 m
+61°2359	170	77.4	2.8	10.56	48 G	.004	74	98	(1.4)
+61°2360	185	77.4	2.9	10.90	56 G	.072	95	119	{2.3}
216629	193	77.2	2.4	9.61	40 G	.076	101	125	2.9 m
+61°2362	197	77.4	2.6	10.46	56 G	.005	151	175	(0.5)
216658	203	77.3	2.3	9.33	40 G	.119	104	128	2.9 m
.....	207	77.3	2.5	11.58	24 G	.059	84	108	(0.8)
.....	208	77.5	2.8	10.92	56 G	.044	91	115	3.2 m
216711	221	77.5	2.7	9.33	56 G	.055	88	112	2.7 m
+61°2365	246	77.6	2.8	9.34	56 G	.033	89	113	2.4 m
216772	258	78.2	4.1	8.64	16 W	.033	167	11	(0.1)
+61°2366	264	77.6	2.8	10.18	56 G	.079	89	113	3.0 m
.....	273	77.6	2.8	10.72	48 G	.032	79	103	2.0 m
.....	294	77.6	2.7	10.88	56 G	.071	95	119	3.0 m
.....	309	77.7	2.7	10.94	48 G	.021	73	97	1.1
+61°2369	326	77.6	2.4	9.33	56 G	.018	65	89	1.0
216898	335	77.6	2.4	8.31	56 G	.083	89	113	2.5 m
216926	348	78.1	3.4	8.88	16 W	.046	68	92	1.0
216945	352	77.6	2.5	(8.13)	56 G	.031	89	113	2.0
+63°1907	384	78.5	4.3	9.78	-	.080	40	64	2.0
217035	385	77.9	2.8	7.90	32 GW	.054	90	114	2.3 m
217061	395	77.8	2.6	9.22	48 G	.042	92	115	2.9 m
217086	405	77.9	2.7	7.98	56 GW	.026	88	111	.....
217174	459	77.8	2.3	8.76	32 G	.032	63	86	1.4
.....	474	77.8	2.3	11.24	32 G	.012	153	176	(0.6)
+61°2377	480	77.9	2.4	10.38	32 G	.023	96	119	(1.2)
217312	520	78.2	3.0	7.53	16 W	.016	84	107	2.0 m
217297	523	78.4	3.5	7.48	16 W	.020	66	89	1.8 m
217463	591	78.2	2.6	9.26	16 W	.038	106	129	2.4 m
217657	690	78.4	2.7	8.27	16 W	.047	36	59	.....
217730	726	78.6	3.0	8.54	16 W	.015	67	89	(1.5)
217796	764	78.3	2.3	8.32	16 W	.007	138	160	(0.8)
217848	789	79.0	3.9	8.60	16 W	.040	119	141	(0.6)
217872	813	78.7	3.0	8.10	16 W	.030	60	82	.....
217918	834	79.1	3.9	8.92	16 W	.061	138	160	(0.1)
217919	841	78.9	3.4	8.71	16 W	.003	31	53	2.7 m
217966	873	78.5	2.3	8.01	16 W	.008	48	70	0.5
217979	875	78.8	3.2	8.72	16 W	.063	115	137	1.8 m
218066	923	78.9	3.0	(7.6)	16 W	.033	46	68	2.1 m
CW Cep						.015	37	59	

HD BD	Brodskaia No.	$\ell^I$	$b^I$	$m_{pg}$	n	p	$\Theta_E$	$\Theta_G$	$A_v$
218139	967	78.9 <sup>o</sup>	+2.9	7.67 <sup>m</sup>	16 W	0.006	76 <sup>o</sup>	98 <sup>o</sup>	(0.6)
218179	995	79.2	3.6	7.81	16 W	.026	48	70	(0.9)
218323	1081	79.4	3.8	7.95	16 W	.020	77	99	2.6 m
218342	1086	79.0	2.8	7.56	16 W	.032	72	94	2.1 m
218363	1106	79.6	4.3	8.93	16 W	.033	76	97	(0.4)
218537	1229	79.4	3.1	(6.39)	-	.014	46	67	0.5
218560	1240	79.6	3.6	7.40	16 W	.003	99	120	.....
+64°1760	1320	79.9	4.2	8.17	16 W	.064	69	90	(0.5)
218672	1330	79.2	2.4	8.04	16 W	.034	149	170	.....
218673	1334	79.2	2.3	8.58	16 W	.031	44	65	(1.8)
218696	1355	79.6	3.4	7.94	16 W	.012	69	90	(0.4)
218723	1365	80.1	4.5	(6.49)	-	.014	172	13	.....
218866	1461	79.9	3.8	7.51	16 W	.012	75	96	(0.8)
219063	1590	80.2	3.9	7.15	16 W	.023	128	148	(0.5)
						.008	159	179	
219126	1650	80.3	4.0	7.20	16 W	.027	64	84	(0.2)
219305	1754	79.8	2.5	8.37	16 W	.008	115	135	(0.0)
219496	1857	80.6	4.1	7.90	16 W	.013	64	84	(0.1)
219523	1884	80.4	3.4	(6.98)	16 W	.012	178	18	.....
						.011	40	60	
219587	1931	80.6	3.9	8.37	16 W	.019	60	79	(-0.1)
219633	1977	80.4	3.2	7.72	16 W	.012	94	113	(1.1)
+63°1962	2037	80.4	2.9	8.49	16 W	.065	62	81	1.7
+63°1964	2053	80.5	3.2	9.02	16 W	.066	61	80	3.0
+62°2210	2167	80.4	2.5	9.32	-	.144	74	93	3.6
220072	2262	81.0	3.8	7.38	16 W	.017	48	67	(0.9)
220208	2375	81.1	3.6	7.17	16 W	.013	92	110	(0.3)
220239	2393	80.9	3.1	8.58	16 W	.023	73	91	(-0.3)
220314	2444	81.1	3.4	7.81	16 W	.024	69	87	(0.0)
+63°1982	2511	81.0	2.8	8.90	16 W	.044	84	102	(-0.1)
220638	2677	81.2	2.7	7.88	16 W	.028	76	94	(1.3)

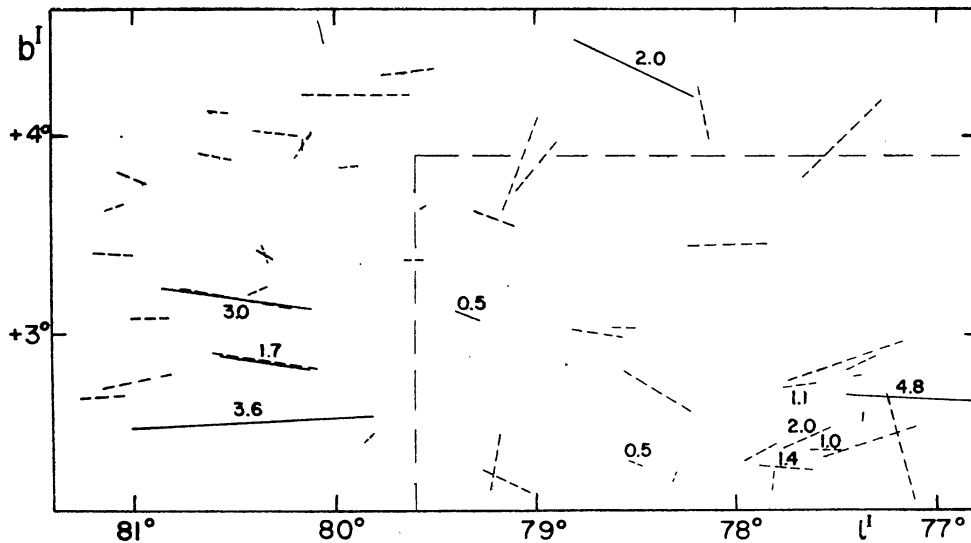


Fig. 4. Similar plot as in Fig. 3, but for probable non-members of the association. The area surrounded by dashed lines is that represented in Fig. 3.

6th gives the total number of exposures for a star. The letter *G* in this column denotes Göttingen plates, the letter *W* Ostrowik plates. In the 7th, 8th and 9th columns the amount of polarization in magnitudes and the position angle of the plane of vibrations in equatorial and galactic co-ordinates are given. The mean photoelectric values from Hall's (1958) catalogue are given in bold type below the photographic values. In the last column the visual absorption derived from data by Blaauw, Hiltner and Johnson (1959) is given; the values obtained from the Brodskaja data are given in parentheses. Johnson's (1958) intrinsic colours *C*<sub>*I*</sub> and the colours *B*—*V* given by Blaauw, Hiltner and Johnson (1959) were used. The letter *m* in the last column of Table 1 denotes the members of the association listed in Table 2 of Blaauw, Hiltner and Johnson's paper.

In Fig. 5 *a* the amount of polarization is plotted against the visual absorption as given by the above authors for the members of the association listed in their Table 2. The open circles denote the photoelectric values of polarization from Hall's catalogue, the crosses denote the photographic values. A similar plot for stars probably not belonging to the association is given in Fig. 5 *b*. The values of the visual absorption obtained from Brodskaja's catalogue were not used in this diagram because of their low accuracy.

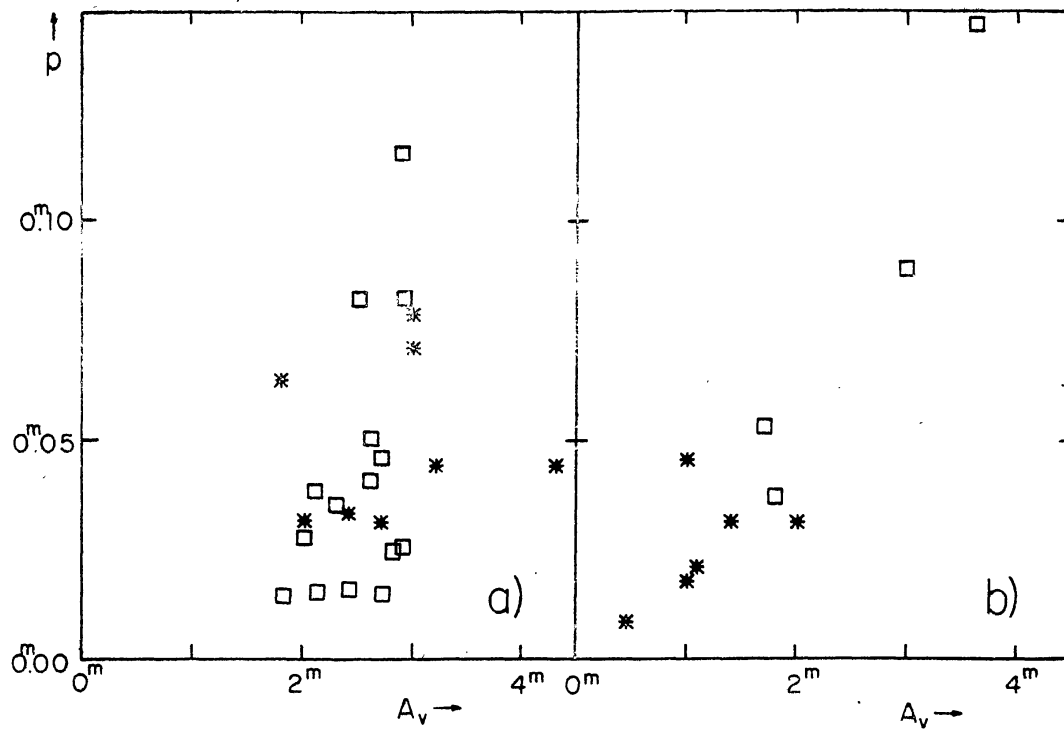


Fig. 5

Fig. 5. Polarization vs. visual absorption a) for members of association III Cephei listed in Table 2 of Blaauw *et al.* (1959), b) for probable non-members of the association; squares denote the photoelectric polarization measurements, asterisks — the photographic ones.

It may be seen that there is a good correlation between polarization and absorption for non-members of the association. The correlation for the members of the association is small which is similar to the case for most other associations and open clusters; the coefficient of correlation computed with taking into account the observational errors is

$$r_{pA} = 0.3 \pm 0.2 \text{ (m. e.)}$$

#### Acknowledgements.

I should like to acknowledge that my interest in the observations of polarization was stimulated by Professor S. L. Piotrowski. I wish also to express my appreciation to Dr M. Karpowicz who made the first experiments with photographic measurements of polarization at Ostrowik in 1954 and to Mr. W. Krzeminski who took part in the first experiments with crossed calcite plates.

Dr. A. Behr and Dr. Th. Schmidt-Kaler have been most helpful in obtaining the polarization plates at Göttingen Observatory. I am indebted to Professor P. ten Bruggencate, Director of Göttingen University Observatory and Professor O. Heckmann, Director of Hamburg-Bergedorf Observatory for placing the facilities of their observatorie at my disposal.

#### REFERENCES

- Bartl, E: 1959 *Mitt. Jena*, Nr. 39.  
 Behr, A: 1955 Les particules solides dans les astres, *Mem. Soc. Roy. Sci. Lège*, IV<sup>e</sup> Serie, **15**, 547.  
 ----- 1956 *Veröff. Göttingen*, Nr. 114.  
 van den Berg, S: 1956 *Zs. f. Ap.*, **40**, 439 = *Veröff. Göttingen*, Nr. 115.  
 Blaauw, A.,  
 Hiltner, W. A.,  
 and Johnson, H. L: 1959 *Ap. J.* **130**, 69 = *Lowell Obs. Reprint*, ser. II, No. 56.  
 Brodskaja, E. S.: 1955 *Izv. Krim. Ap. Obs.*, **14**.  
 Gossner, J. L.: 1952 *A. J.*, **57**, 11.  
 Hall, J. S.: 1958 *Publ. U. S. Naval Obs.*, **17**, Part VI.  
 Johnson, H. L.: 1958 *Lowell Obs. Bult.*, **4** (No. 90), 37.  
 Loden, L. O.: 1958 *Arkiv f. Astr.*, **2**, 111.  
 Markowitz, Wm.,  
 and Hall, J. S.: 1950 *A. J.*, **55**, 175.  
 Markowitz, Wm.: 1951 *A. J.*, **56**, 139.  
 Serkowski, K.: 1958 a *Postępy Astronomii* (Cracow), **6**, 160.  
 ----- 1958 b *Acta Astr.*, **8**, 135 (Appendix 1) = *Warsaw Repr.*, No. 72

University of Warsaw, Astronomical Observatory and  
 Polish Academy of Sciences, Institute of Astronomy  
 May, 1960.

K. Serkowski.

## Photoelectric Observations of Magnetic Stars

by

T. Jarzębowski

### SUMMARY

This paper (being the continuation of papers [2], [9]) contains the results of additional photometric observations of 53 Cam and HD 71866 and new results of HD 32633, HD 200311 and HD 215038.

53 Cam shows periodic variations in luminosity in blue and yellow with the mean amplitude 0<sup>m</sup>015. There exists a phase shift of the order of 0<sup>d</sup>2 *P* between light curves for these two colors.

HD 71866 shows periodic variations with a mean amplitude of 0<sup>m</sup>035 in blue, 0<sup>m</sup>015 in yellow.

HD 32633 and HD 200311 show irregular variations in luminosity.

The light of HD 215038 varies probably periodically with an amplitude of the order 0<sup>m</sup>1 and period 1<sup>d</sup>97.

### 53 Cam (HD 65339)

The period of magnetic variations of this star, according to new data obtained by H. W. Babcock [1], is 8<sup>d</sup>0248.

The preliminary results of photometric observations of the star made in 1959 were already published in [2], [8]; light variations with a period of 8<sup>d</sup>0 and amplitude 0<sup>m</sup>015 were stated in  $\lambda_{\text{eff}} = 4200$ .

In the present investigation the star has been studied on 27 nights (970 comparisons) in two colors, their effective wave lengths corresponding to  $\lambda_{\text{eff}} = 4200$  and  $\lambda_{\text{eff}} = 5350$ . The method of observations was already described in [2]. The newly obtained results are listed in Table 1; (the magnitude differences between the comparison star (HD 65301) and 53 Cam are mean values; the number of comparisons from which this mean was taken is denoted by *n*). The magnitude differences HD 65301 — 53 Cam are plotted in Fig. 1 for a period of 8<sup>d</sup>0248.

The photometric results obtained in  $\lambda_{\text{eff}} = 4200$  distinctly confirm those of 1959 (plotted also in the Figure). The joint results in  $\lambda_{\text{eff}} = 4200$  furnish the following elements of light variation: Minimum light = JD 2437002<sup>d</sup>4 + 8<sup>d</sup>024 *E*.

The results obtained in  $\lambda_{\text{eff}} = 5350$  indicate that the amplitude in this wave length is of the same order (0<sup>m</sup>015). There is, however, a considerable phase shift — the minimum in  $\lambda_{\text{eff}} = 5350$  occurring about 0<sup>d</sup>2 *P* later than in  $\lambda_{\text{eff}} = 4200$ . A difference in the shape of the curves for these two colors also seems to exist.

Table I  
53 Cam

$\lambda_{\text{eff}} = 5350$					
JD 2430000 +	n	HD 65301 - - 53 Cam	JD 2430000 +	n	HD 65301 - - 53 Cam
6669.30	12	-0 <sup>m</sup> .269 ± 0.004	7018.37	18	-0 <sup>m</sup> .273 ± 0.003
6672.29	12	.268 .003	7021.35	24	.281 ,002
6673.29	15	.278 .002	7026.37	18	.276 .001
6675.28	15	.283 .003	7052.32	30	.277 .003
6957.44	15	.273 .004	7053.33	30	.281 .002
6967.40	12	.264 .004	7057.34	29	.264 .003
6968.40	18	.263 .002	7058.32	18	.276 ,003
6969.37	12	.270 .002	7059.33	29	.275 .004
7002.40	30	.272 .002	7060.34	37	.276 .003
7016.36	18	.266 ..002			

$\lambda_{\text{eff}} = 4200$					
JD 2430000 +	n	HD 65301 - - 53 Cam	JD 2430000 +	n	HD 65301 - - 53 Cam
6957.40	18	+0 <sup>m</sup> .006 ± 0.002	7016.33	21	+0 <sup>m</sup> .005 ± 0.001
6958.32	12	+0.004 .006	7016.38	18	+0.003 .002
6959.54	26	+0.001 .002	7017.33	24	+0.001 .001
6967.38	12	+0.003 .003	7018.28	18	-0.003 .004
6968.36	24	+0.004 .002	7018.34	18	-0.013 .002
6969.34	26	-0.002 .003	7018.41	18	-0.006 .001
6970.33	36	-0.005 .001	7019.38	18	-0.001 .003
6971.34	24	-0.002 .002	7021.33	18	+0.005 ,002
7002.30	18	-0.012 .003	7021.37	21	+0.007 .001
7002.42	24	-0.011 .002	7025.36	28	+0.001 .002
7003.30	15	-0.007 .003	7026.34	29	-0.008 .001
7003.39	21	-0.009 .002	7026.38	18	-0.006 .002
7008.27	23	-0.001 .002	7027.34	24	-0.002 .002
7016.32	14	+0.008 .004	7028.35	18	+0.003 .001

In the lower part of Fig. I the curve of the mean color index is plotted. The magnetic curve of the star, recently received from H. W. Babcock [1], is plotted in the upper part of Fig. I.

A comparison of magnetic variation and light variation seems to indicate that the phase of maximum negative magnetic field falls

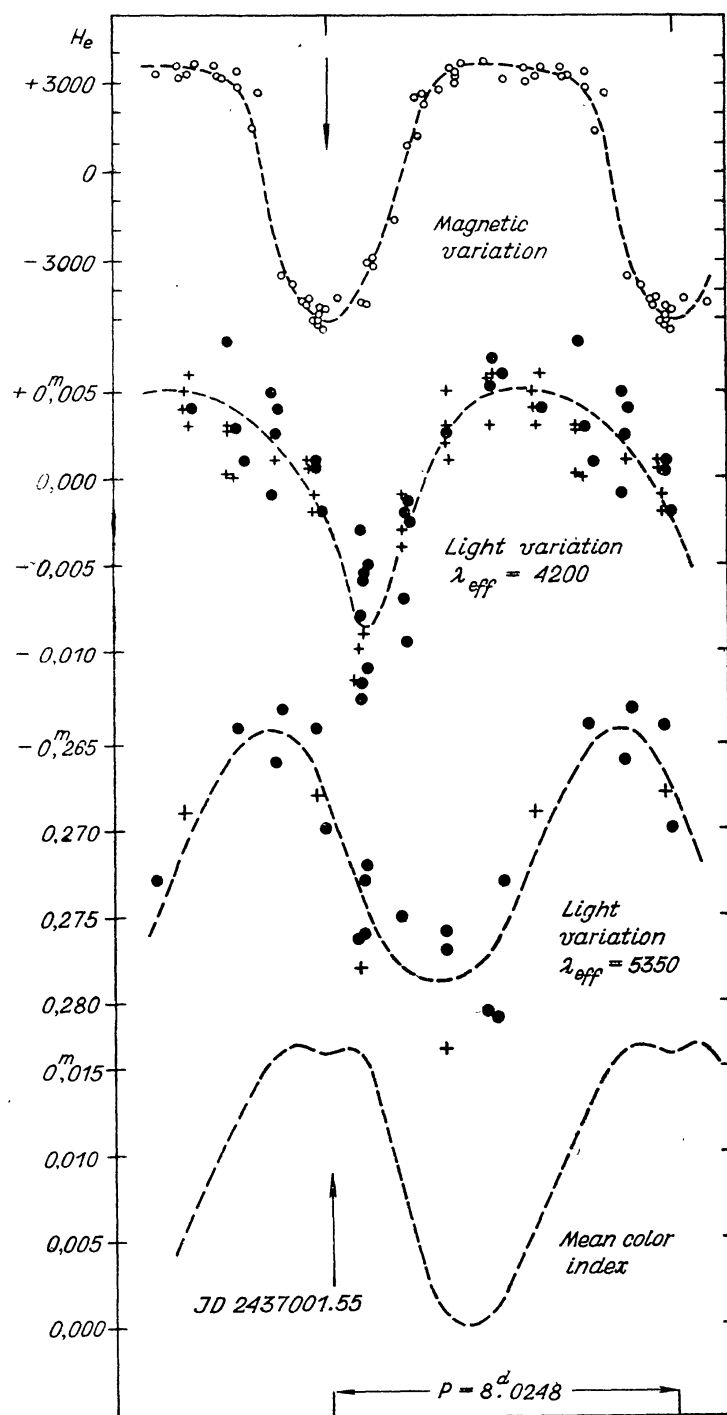


Fig. 1. Comparison of magnetic variation, light variation and variation of the color index in 53 Cam.

Dots — photometric measurements of 1960, crosses — those of 1959.

near the phase of minimum light for  $\lambda_{\text{eff}} = 4200$  and near the phase of maximum light for  $\lambda_{\text{eff}} = 5350$ . Thus, in the case of this star the phase relationship between magnetic variation and light variation is much more complicated than supposed in [2], [3]. It should be noted,

however, that the extremes of the color index approximately coincide with the extremes of the field. Maximum color index occurs at the time of maximum negative magnetic field.

The observations of this star will be continued in three colors. If future observations confirm this phase shift, this phenomenon may be interpreted as a real argument in favour of the oscillator theory and against the oblique rotator theory.

### HD 71866

The magnetic field of the star varies with a period of  $6^d799$  [4]. The light variation of this star has been studied by the author in 1959; for  $\lambda_{\text{eff}} = 4200$  he found periodic variations with the same period and an amplitude of  $0^m037$  [2], [3], [5].

In the present investigation the star has been studied in two colors during 28 nights (800 comparisons). These new results are listed in Table 2 and plotted for a period of  $6^d799$  in Fig. 2, where, for comparison, the results of 1959 are also plotted (crosses).

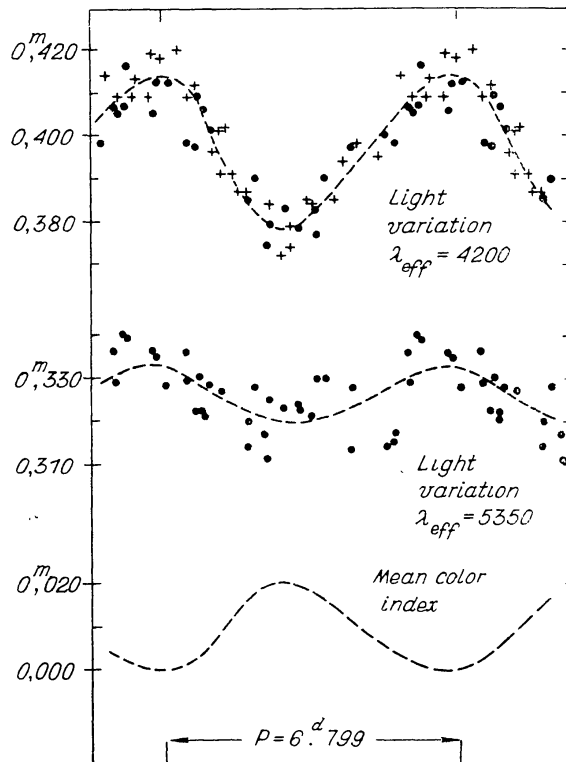


Fig. 2. Light variation of HD 71866. Dots — the results of 1960, crosses — the results of 1959.

The results in  $\lambda_{\text{eff}} = 4200$  confirm those of 1959; the mean amplitude of light variation for this effective wave length is  $0^m035$ . The epoch of minimum light:  $\text{JD } 24\,36998.50 + 6^d799 E$ .

The amplitude of light variation in  $\lambda_{\text{eff}} = 5350$  is much smaller, being of the order of  $0^m015$ ; there is, however, a large random dispersion for individual nights which is probably physically real.

Table 2  
HD 71866

$\lambda_{\text{eff}} \approx 6360$					
JD 2430000 +	n	HD 71844 - - HD 71866	JD 2430000 +	n	HD 71844 - - HD 71866
6957.49	15	<sup>m</sup> 0.325 ± 0.002	7019.33	15	<sup>m</sup> 0.324 ± 0.005
6967.44	12	.336 .004	7021.34	27	.314 .003
6968.47	18	.335 .003	7025.32	17	.317 .003
6969.43	15	.330 .004	7025.40	18	.311 .002
6971.40	15	.323 .004	7026.42	12	.321 .003
6972.33	12	.330 .005	7027.33	30	.313 .003
6981.34	18	.339 .004	7028.31	18	.315 .003
6996.36	18	.329 .006	7028.38	18	.317 .003
6999.34	12	.330 .003	7030.30	18	.336 .005
7002.36	10	.336 .004	7044.31	14	.322 .002
7003.35	12	.322 .004	7044.35	12	.321 .003
7008.31	18	.329 .002	7045.33	15	.314 .002
7015.27	18	.340 .005	7045.36	12	.320 .003
7016.28	15	.328 .002	7053.37	16	.323 .005
7017.28	18	.328 .003	7058.35	18	.327 .003
7018.31	15	.328 .004	7061.34	30	.328 .003

$\lambda_{\text{eff}} \approx 4200$					
JD 2430000 +	n	HD 71844 - - HD 71866	JD 2430000 +	n	HD 71844 - - HD 71866
6957.47	15	<sup>m</sup> 0.379 ± 0.003	7015.29	9	<sup>m</sup> 0.407 ± 0.004
6967.43	12	.406 .003	7016.30	12	.412 .002
6968.43	18	.412 .002	7017.30	12	.401 .005
6969.40	15	.409 .003	7018.32	10	.390 .003
6971.39	15	.383 .002	7019.35	10	.378 .004
6972.31	12	.390 .002	7021.30	9	.400 .002
6981.32	6	.416 .001	7025.41	12	.374 .004
6996.36	12	.398 .005	7026.43	6	.383 .003
6999.34	12	.377 .002	7027.31	12	.397 .003
7002.38	10	.405 .004	7028.33	12	.398 .003
7003.33	10	.397 .004	7044.33	12	.406 .003
7008.33	12	.405 .003	7045.36	10	.385 .003

A comparison of magnetic variation and light variation confirms the conclusion obtained in 1959 [<sup>2</sup>], [<sup>3</sup>], [<sup>5</sup>]: for  $\lambda_{\text{eff}} = 4200$  the phase of minimum light coincides strongly with the phase of maximum positive magnetic field; for  $\lambda_{\text{eff}} = 5350$  a similar relationship seems also to exist. The phase of maximum color index coincides with the phase of maximum positive magnetic field — thus inversely than in the case of 53 Cam.

### HD 32633

The star has been investigated during 28 nights: 15 nights in 1960 and 13 in 1959. The measurements were only made in  $\lambda_{\text{eff}} = 4200$ .

Table 3  
HD 32633

1959			1960		
JD 2436000 +	n	HD 32608 - - HD 32633	JD 2436000 +	n	HD 32608 - - HD 32633
573.33	13	-0 <sup>m</sup> .389 ± 0.005	957.34	15	-0 <sup>m</sup> .385 ± 0.002
585.33	9	.400 .000	958.29	12	.397 .005
609.31	8	.406 .005	965.35	11	.370 .003
613.26	17	.390 .008	966.33	9	.357 .005
614.26	15	.400 .006	967.34	9	.370 .003
616.27	14	.410 .006	968.31	18	.370 .002
622.35	9	.400 .006	969.29	13	.385 .003
628.31	13	.400 .004	970.25	9	.384 .003
629.22	8	.440 .007	971.26	13	.377 .003
629.26	9	.396 .008	972.28	7	.366 .004
630.25	18	.400 .003	981.29	18	.374 .003
631.25	14	.390 .004	996.31	11	.388 .004
637.25	15	.385 .002	999.30	13	.376 .004
638.28	17	.358 .004	1002.26	13	.399 .003
			1003.26	15	.391 .003

JD 2436000 +	n	HD 32608 - - HD 32574	JD 2436000 +	n	HD 32608 - - HD 32574
957.34	10	-1 <sup>m</sup> .064 ± 0.003	971.26	6	-1 <sup>m</sup> .068 ± 0.003
958.29	6	1.069 .006	972.28	4	1.064 .005
965.33	8	1.064 .002	981.29	6	1.066 .001
966.33	6	1.068 .004	996.31	7	1.064 .006
967.34	4	1.069 .003	999.30	6	1.055 .005
968.31	6	1.068 .003	1002.26	6	1.060 .007
969.29	6	1.064 .006	1003.26	6	1.060 .003
970.25	4	1.065 .001			

As comparison star HD 32608 has been used. The relative values of extinction were determined for every night using the method described in [2] (for HD 153882) — the corresponding corrections for extinction did not exceed  $0.^m002$ . To test the constancy of light of the comparison star simultaneous measurements of the differences HD 32608 — HD 32574 were made (in 1960 only).

The results of the measurements are listed in Table 3. In the lower part of this Table the mentioned magnitude differences HD 32608 — HD 32574 are listed, which show the constancy of light of the comparison star.

The obtained magnitude differences HD 32608 — HD 32633 indicate that HD 32633 shows small variations in luminosity of the order of a few hundredths of a magnitude. It should also be noted that the mean value of the difference HD 32633 — HD 32608 was  $0.^m397$  in 1959 while  $0.^m379$  in 1960 (this difference was not caused by any instrumental change, because the results obtained in the case of 53 Cam and HD 71866 (observed in the same time) show no systematic differences).

The variations of light of this star are probably not periodic. The observations of 1960 could eventually be satisfied by the period  $5.^d5$  which, however, does not satisfy the results of 1959. The value of the period  $4.^d0$  (previously assumed value of the period of magnetic variation [4]) is also excluded. Therefore one can suppose that the light of the star varies irregularly, similarly as its magnetic field [6].

### HD 200311

This star has been investigated in  $\lambda_{\text{eff}} = 4200$  during 9 nights (280 comparisons). Three comparison stars were used: HD 200407, HD 200103 and HD 200020. In Table 4 the magnitude differences

Table 4

HD 200311

JD 2436000 +	n	HD 200407 - - HD 200311	JD 2436000 +	n	HD 200407 - - HD 200311
893.21	16	$-0.^m663 \pm 0.004$	903.21	16	$-0.^m624 \pm 0.003$
896.20	24	.637 .007	919.18	19	.640 .004
897.21	16	.631 .003	920.18	15	.639 .003
898.21	18	.636 .004	930.21	11	.626 .004
899.20	18	.634 .003			

HD 200407 — HD 200311 are given. The joint results of photometric observations indicate possible (rather irregular) variations in luminosity of small amplitude. The variations of the magnetic field of this star are not yet known.

According to the HD Catalogue the magnitude of the star is  $7^m.9$  (spectral type A0). This value is not correct. The magnitude differences measured between this star and the three mentioned comparison stars indicate that the magnitude of HD 200311 must be  $7^d.4$  — instead of the value  $7^d.9$  given in the Catalogue; the magnitude differences measured by our apparatus agree with the photographic and photovisual ones [7].

### HD 215038

This star has been investigated in  $\lambda_{\text{eff}} = 4200$  during 21 nights (300 comparisons). As comparison star HD 214710 was used (situated only about  $15'$  from HD 215038). The results listed in Table 5 indicate

Table 5

HD 215038

JD 2436000 +	n	HD 214710 - - HD 215038 (+ const.)	JD 2436000 +	n	HD 214710 - - HD 215038 (+ const.)
899.34	18	$0^m.020 \pm 0.006$	969.24	18	$0^m.075 \pm 0.004$
920.23	12	.076 .005	970.23	12	.036 .006
930.24	6	.088 .006	971.23	17	.110 .005
956.27	18	.040 .005	972.25	15	.049 .006
957.30	18	.070 .004	973.23	12	.115 .006
958.26	12	.034 .004	981.25	15	.085 .004
960.29	6	.020 .007	982.70	3	.003 .013
965.30	13	.097 .006	987.68	12	.057 .004
966.31	13	.034 .007	996.27	15	.000 .007
967.31	12	.076 .005	999.26	18	.018 .005
968.24	18	.037 .004	999.65	18	.062 .007

variations in luminosity of the order of  $0^m.1$ . The variations may be satisfied by the period  $1^d.97$ ; (the constancy of light of the comparison star was not tested — there is, however, low probability that a star of this spectral type (K5) would have so short a period). More detailed observations of this star will be continued.

According to the new data obtained by Babcock [8] the magnetic field of this star shows always the same polarity without indication of periodicity. If future observations confirm the periodicity of its luminosity variations, this star will present a similar case as HD 215441 [9], HD 224801 or 73 Dra.

I would like to thank Dr. H. W. Babcock for the communication of the recent data of his researches, particularly for the new elements of magnetic variation and magnetic curve of 53 Cam.

## REFERENCES:

- [1] H. W. Babcock: Private communication.
- [2] T. Jarzębowski: *Acta Astronomica* **10**, 31, 1960.
- [3] T. Jarzębowski: *Kleine Veröffentlichungen der Remeis-Sternwarte Bamberg*, Nr. 27, 35, 1960.
- [4] H. W. Babcock: *Ap. J.* **128**, 228, 1958.
- [5] T. Jarzębowski: *P. A. S. P.*, **72**, 123, 1960.
- [6] H. W. Babcock: Private communication.
- [7] E. Rybka: *Acta Astronomica*, sér. c, **5**, 40, 1953.
- [8] H. W. Babcock: Private communication.
- [9] T. Jarzębowski: *Acta Astronomica*, **10**, 119, 1960.

Wrocław Observatory, June 1960.

T. Jarzębowski